Structural basis of orientated asymmetry in a mGlu heterodimer

Weizhu Huang[1,2,*], Nan Jin[1,2,3,*], Jia Guo[3,4,*], Cangsong Shen[1,2,3,*], Chanjuan Xu[1,2,5,*], Kun Xi[3,*], Léo Bonhomme[6], Robert B. Quast[6], Dan-Dan Shen[3,4], Jiao Qin[3,4], Yi-Ru Liu[1,2], Yuxuan Song[1,2], Yang Gao[4], Emmanuel Margeat[6], Philippe Rondard[7], Jean-Philippe Pin[7,#], Yan Zhang[3,4,8,9,#], Jianfeng Liu[1,2,5,#]

[1] Key Laboratory of Molecular Biophysics of MOE, College of Life Science and Technology, Huazhong University of Science and Technology (HUST), Wuhan, 430074, China

[2] International Research Center for Sensory Biology and Technology of MOST, College of Life Science and Technology, Huazhong University of Science and Technology (HUST), Wuhan, 430074, China

[3] Department of Biophysics and Department of Pathology of Sir Run Run Shaw Hospital, Zhejiang University School of Medicine, Hangzhou 310058, China.

[4] Liangzhu Laboratory, Zhejiang University, Hangzhou 311121, China

[5] Bioland Laboratory, Guangzhou Regenerative Medicine and Health Guangdong Laboratory, Guangzhou 510005, China

[6] Centre de Biologie Structurale (CBS), Univ. Montpellier, CNRS, INSERM, Montpellier, France

[7] Institut de Génomique Fonctionnelle (IGF), Univ. Montpellier, CNRS, INSERM, 34094 Montpellier, France

[8] Center for Structural Pharmacology and Therapeutics Development, Sir Run Run Shaw Hospital, Zhejiang University School of Medicine, Hangzhou 310016, China

[9] MOE Frontier Science Center for Brain Research and Brain-Machine Integration, Zhejiang University School of Medicine, Hangzhou 310058, China

[*] These authors contributed equally to this work.

[#] Co-corresponding authors: Jianfeng Liu (jfliu@mail.hust.edu.cn)
Yan Zhang (zhang_yan@zju.edu.cn)
Jean-Philippe Pin (jean-philippe.pin@igf.cnrs.fr)

Supplementary Figures

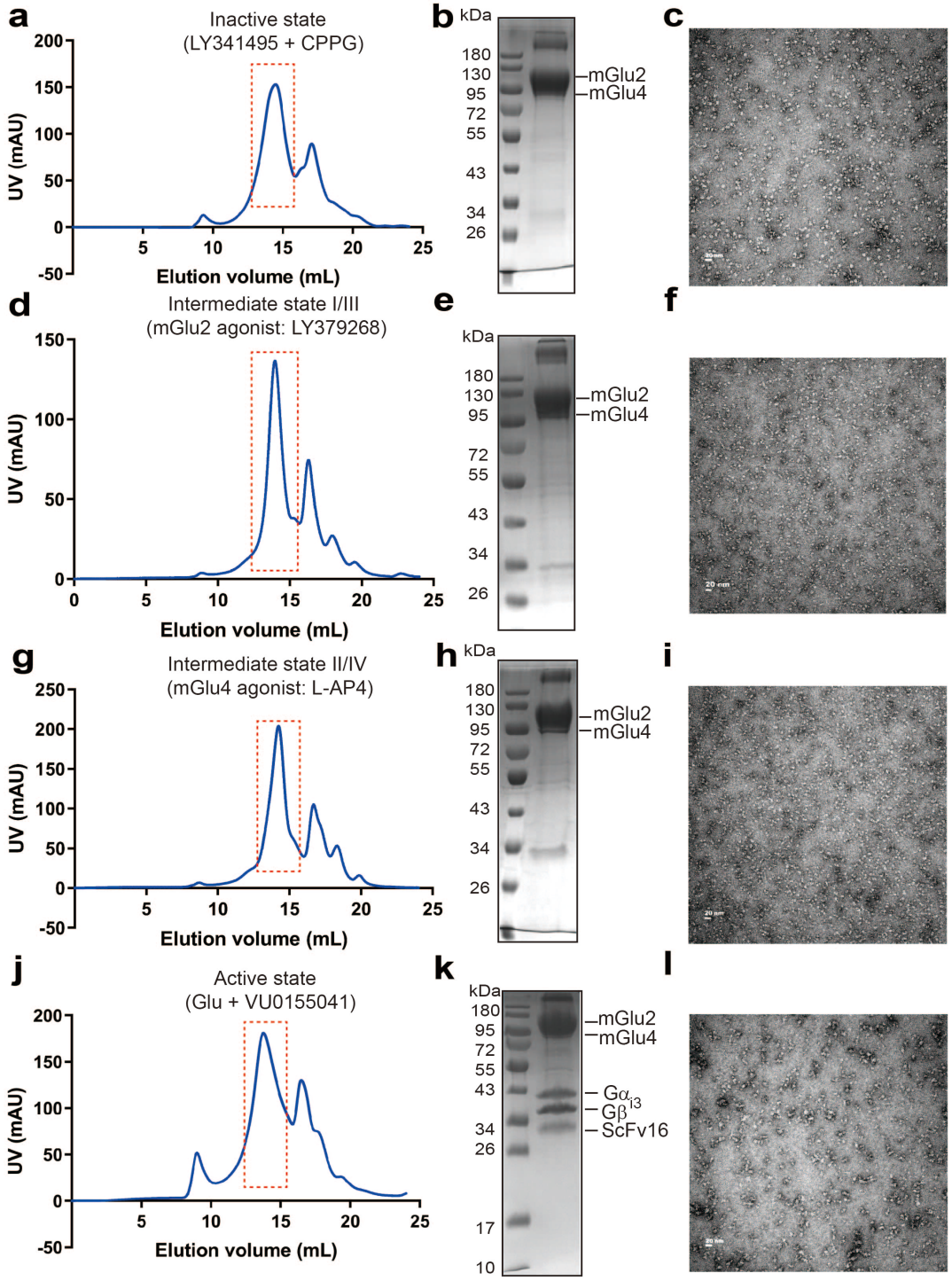

Supplementary Fig. 1. Sample preparation of mGlu2-4 heterodimer. a-i, Size-exclusion chromatography (SEC) profiles *(a, d, g, j)*, SDS-PAGE (Coomassie blue stain) *(b, e, h, k)* and negative-staining electron microscopy analysis *(c, f, i, l)* of the purified mGlu2-4 heterodimer in inactive state, intermediate state (mGlu2 agonist or mGlu4 agonist) and G protein-coupled state.

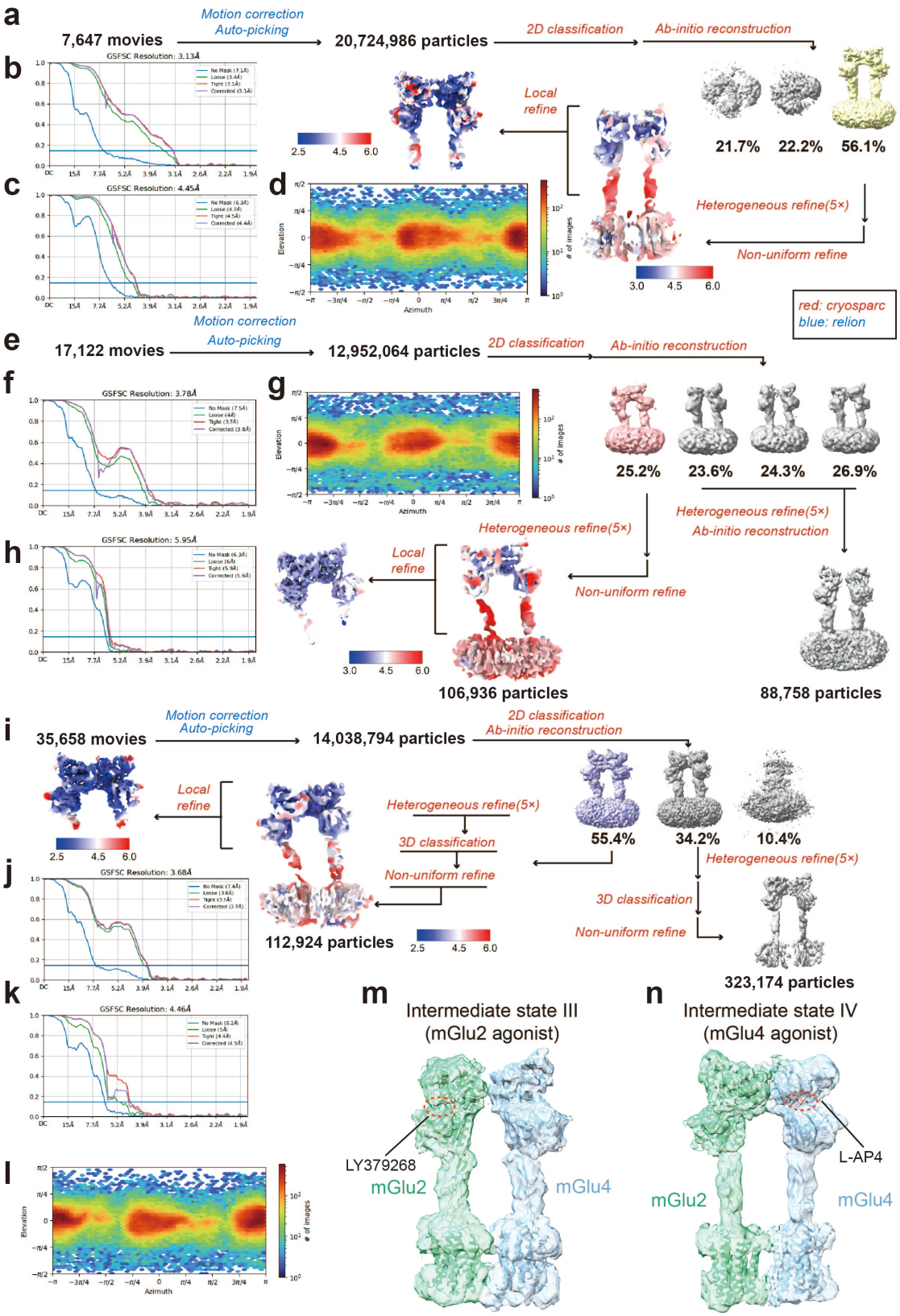

Supplementary Fig. 2. Flow chart of single-particle cryo-EM data processing of inactive state and intermediate state of mGlu2-4 heterodimer. a, Cryo-EM data processing workflow for the inactive state of mGlu2-4 heterodimer. **b-c**, Fourier shell correlation (FSC) curve for the inactive state mGlu2-4 heterodimer cryo-EM map of the VFT **(b)** and the global refinement **(c)**. Dashed lines represent the

resolution at 0.143 FSC. **d,** Angular distribution heat map of particles for reconstruction of the inactive state mGlu2-4 heterodimer. **e**, Cryo-EM data processing workflow for the intermediate states (mGlu2 agonist) mGlu2-4 heterodimer. **f-g**, FSC curve for the intermediate state (mGlu2 agonist) mGlu2-4 heterodimer cryo-EM map of the VFT **(f)** and global **(g)** refinement. **h**, Angular distribution heat map of particles for reconstruction of the intermediate state (mGlu2 agonist) mGlu2-4 heterodimer. **i**, Cryo-EM data processing workflow for the intermediate state (mGlu4 agonist) mGlu2-4 heterodimer. **j-k**, FSC curve for the intermediate state (mGlu4 agonist) mGlu2-4 heterodimer cryo-EM map of the VFT **(j)** and global **(k)** refinement. **l**, Angular distribution heat map of particles for reconstruction of the intermediate state (mGlu4 agonist) mGlu2-4 heterodimer. **m-n**, Cryo-EM maps and overall structures of the intermediate state III (mGlu2 agonist) **(m)** or intermediate state IV (mGlu4 agonist) **(n)** of mGlu2-4 heterodimer.

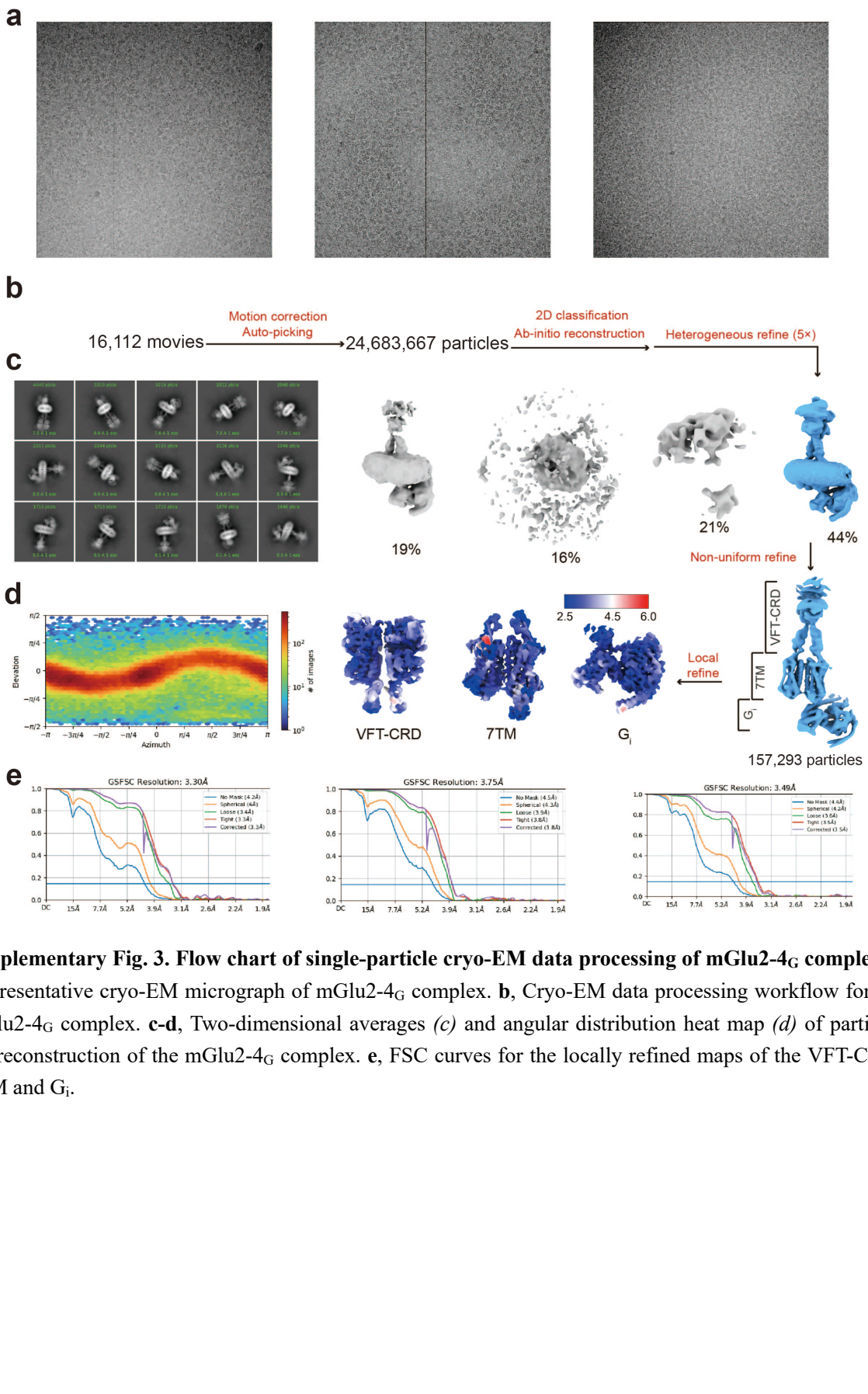

Supplementary Fig. 3. Flow chart of single-particle cryo-EM data processing of mGlu2-4$_G$ complex. a, Representative cryo-EM micrograph of mGlu2-4$_G$ complex. **b**, Cryo-EM data processing workflow for the mGlu2-4$_G$ complex. **c-d**, Two-dimensional averages *(c)* and angular distribution heat map *(d)* of particles for reconstruction of the mGlu2-4$_G$ complex. **e**, FSC curves for the locally refined maps of the VFT-CRD, 7TM and G_i.

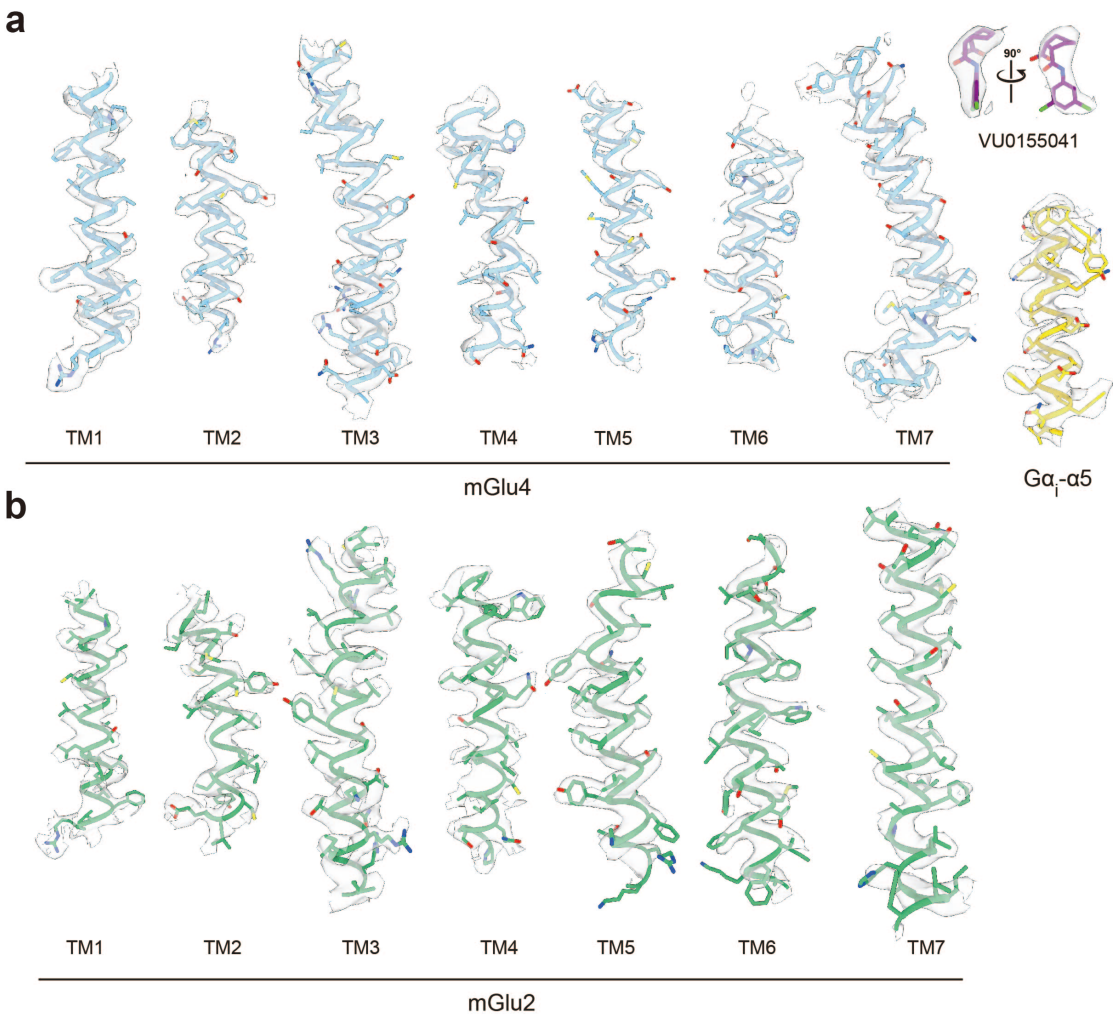

Supplementary Fig. 4. Agreement between cryo-EM maps and models of mGlu2-4$_G$ complex. a-b, EM density and model for the mGlu2 subunit *(a)* and mGlu4 subunit *(b)* in mGlu2-4$_G$ complex are shown for transmembrane helices, mGlu4 PAM VU0155041 and α_5 helix of Gα_i.

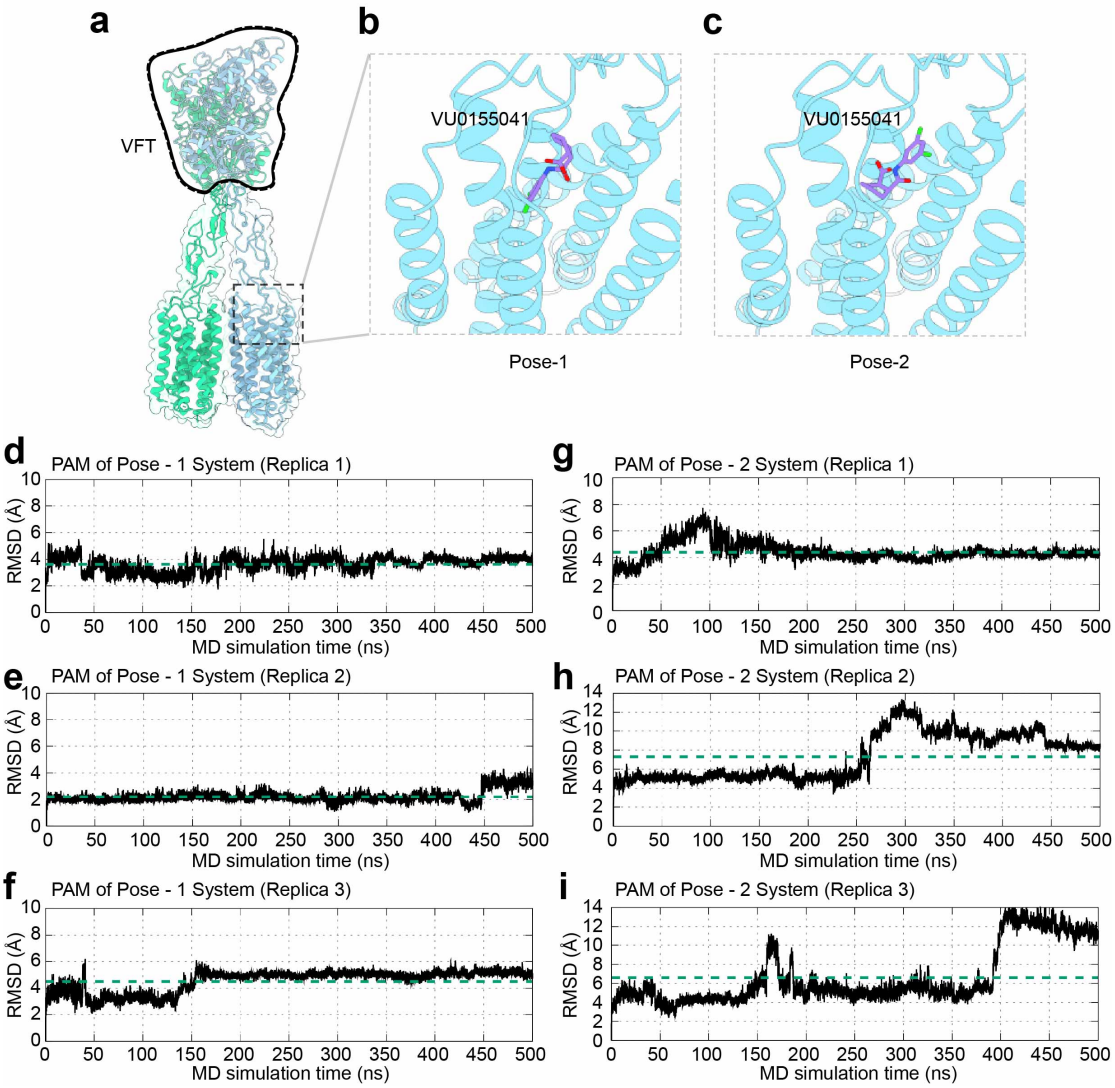

Supplementary Fig. 5. The mGlu2-4 heterodimer complex with different pose of VU0155041 used for MD simulation and the calculation results. a-c, Side view of the mGlu2-4 heterodimer complex with the removal of the VFT domain *(a)*, which was used as input model for MD simulation to evaluate the binding stability of two possible poses of VU0155041 (recognized as PAM): Pose-1 with an inward-facing aromatic ring *(b)* and Pose-2 with an outward-facing aromatic ring *(c)*. **d-i**, The RMSD of PAM for the three replicates of the Pose-1 *(d-f)* and the Pose-2 *(g-i)* systems along the MD simulation time.

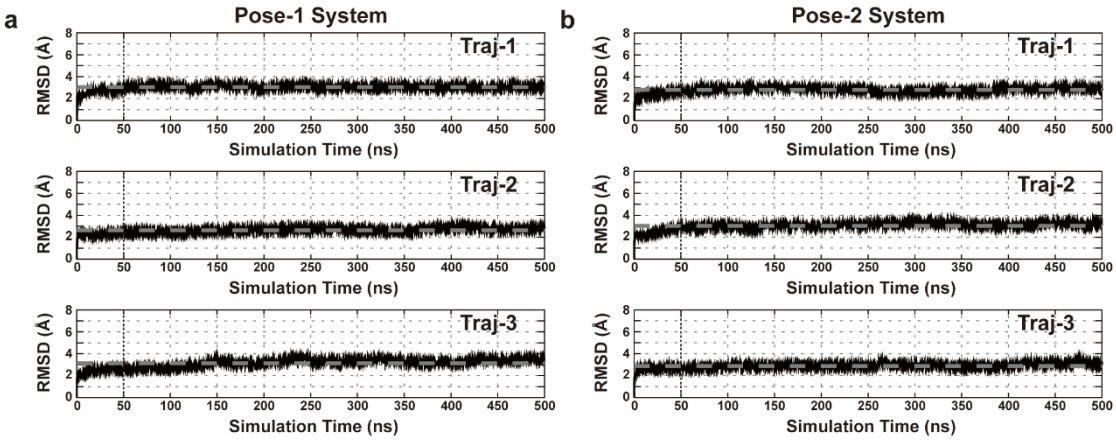

Supplementary Fig. 6. Stability evaluation of MD simulations. a-b, The RMSD of all heavy atoms of mGlu2-4 heterodimer complex (except the loops in the extracellular and intracellular regions) for the three replicas of Pose-1 system *(a)* and Pose-2 system *(b)*.

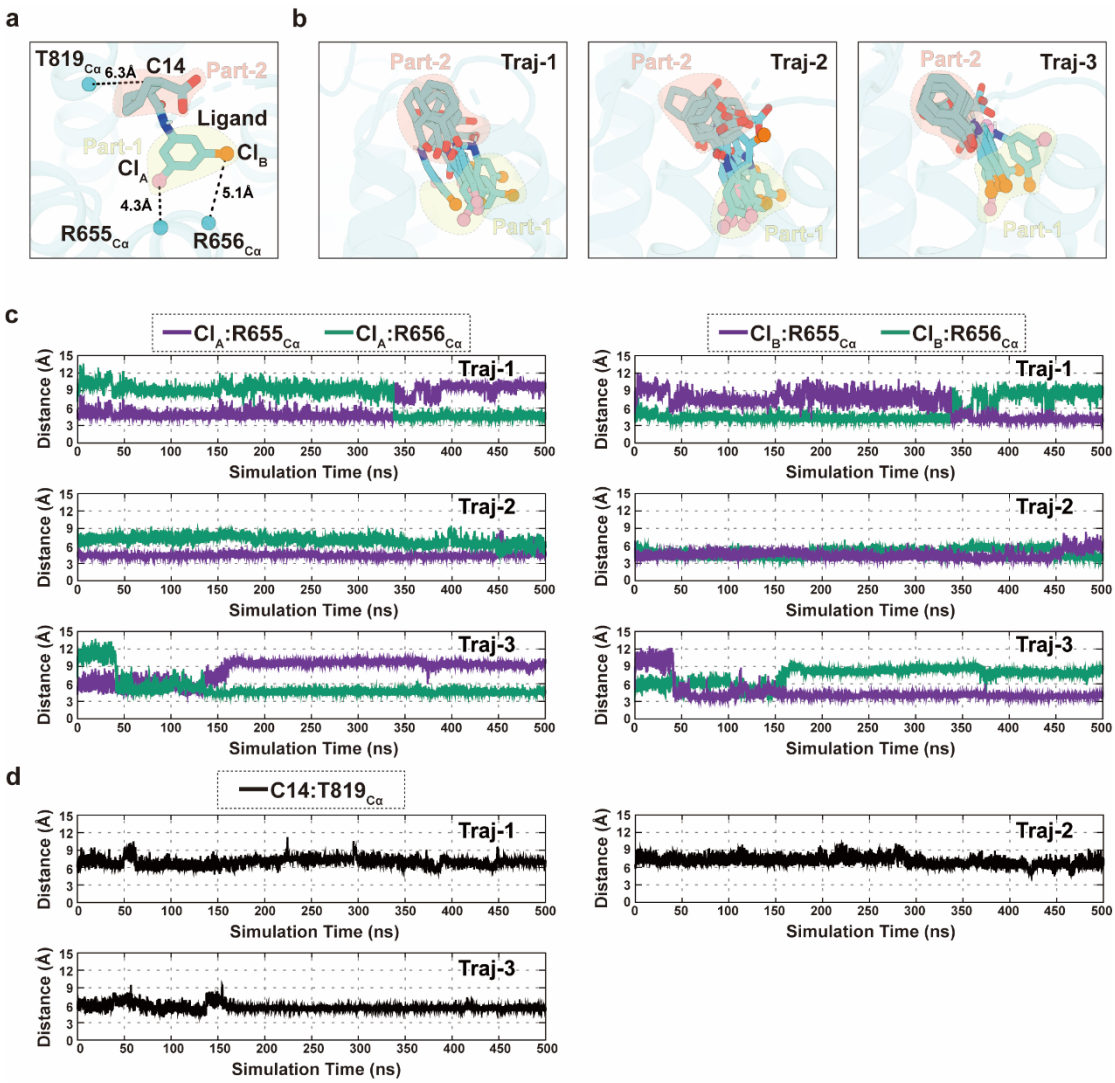

Supplementary Fig. 7. Ligand pose stability evaluated for Pose-1 systems. a, Important contacts used to evaluate the stability of the ligand pose: the distances between the chloride atoms (Cl_A and Cl_B) and the Cα atoms of R655/R656 (Part-1 of ligand), the distance between the C14 of ligand and the Cα atom of T819 (Part-2 of ligand). **b**, Snapshots of representative conformations (saved every 100 ns for each trajectory) of the three replicas of pose-1 MD simulations. **c-d,** Distance distribution of the important contacts to monitor the pose stability of ligand for the three replicas of pose-1 MD simulation.

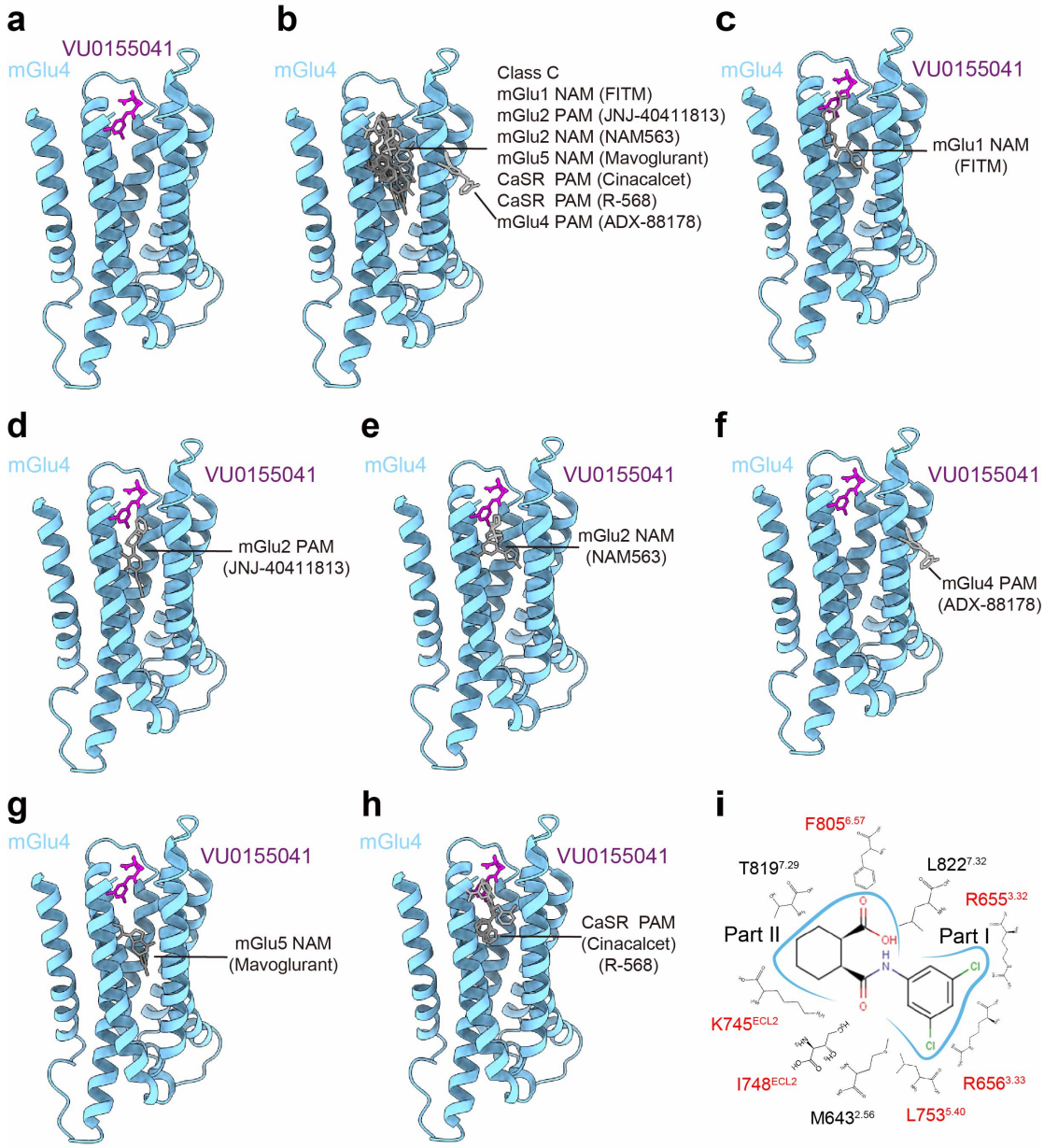

Supplementary Fig. 8. Comparison of the PAM binding pocket in the structures of the indicated class C GPCRs. a, VU0155041 binding mode in mGlu4 subunit of mGlu2-4_G complex. **b,** Overlap of binding pocket of the reported class C GPCR allosteric molecules and VU0155041 in mGlu4 subunit in mGlu2-4_G complex. **c-h**, VU0155041 binding pocket compared with mGlu1 NAM FITM (PDB: 4OR2) *(c)*, mGlu2 PAM JNJ-40411813/ADX-71149 (PDB: 8JD5) *(d)*, mGlu2 NAM NAM563 (PDB: 7EPE) *(e)*, mGlu4 PAM ADX-88178 (PDB: 8JD5) *(f)*, mGlu5 NAM Mavoglurant (PDB: 4OO9) *(g)*, and CaSR PAM Cinacalcet (PDB: 7M3F) and R-568 (PDB: 9AVL) *(h)*. **i**, Detailed binding mode of VU0155041 in mGlu4 subunit.

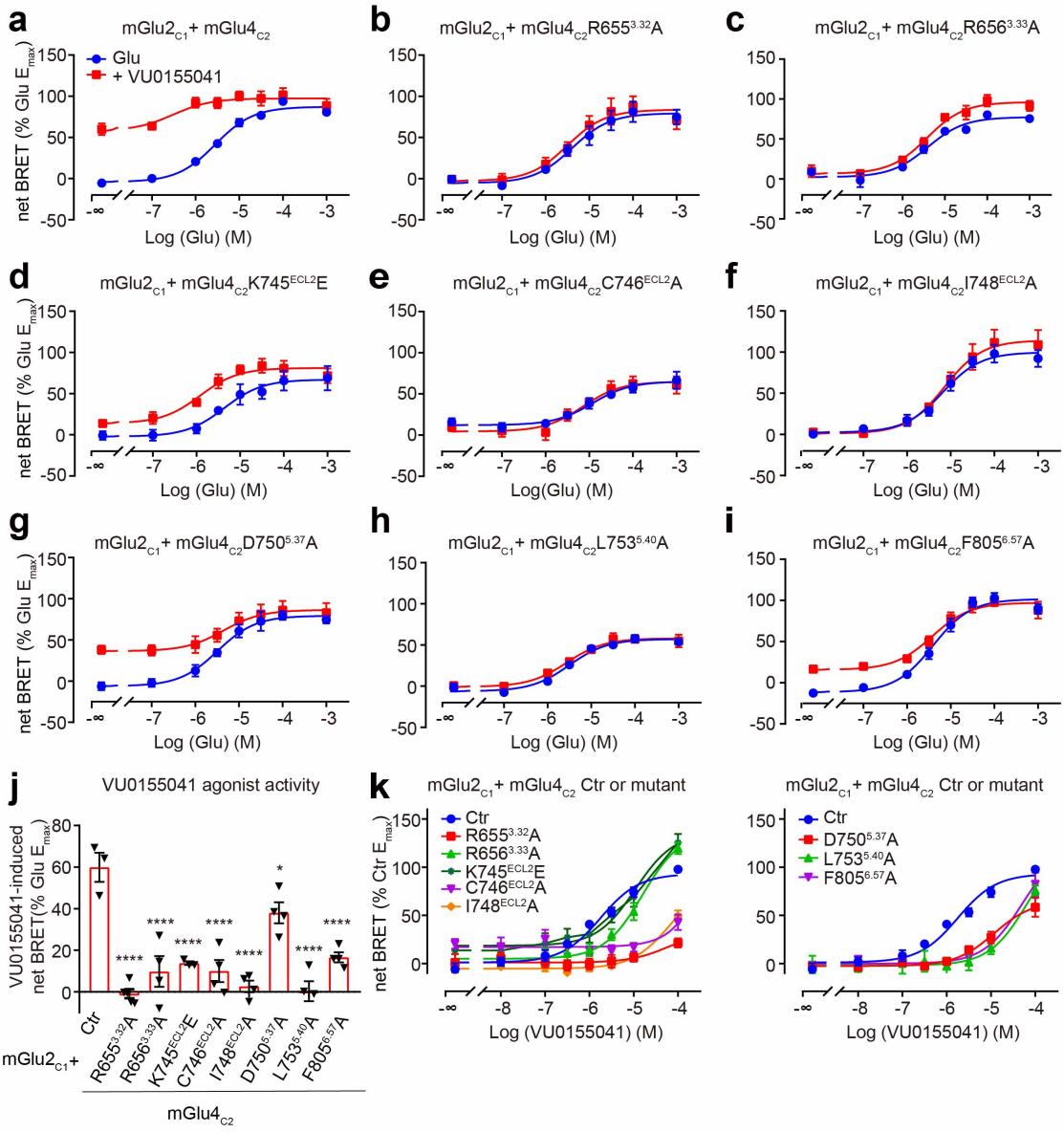

Supplementary Fig. 9. The binding pocket of VU0155041 in mGlu4 subunit of mGlu2-4 heterodimer. **a-i**, Dose response curves of Glu with or without VU0155041 (3.16 μM) for G protein activation in mGlu2$_{C1}$-mGlu4$_{C2}$ heterodimer without or with the mutation of the indicated residues of the binding pocket of VU0155041. Data are normalized by using the maximum response (E_{max}) of Glu in the cells transfected with mGlu2$_{C1}$ and mGlu4$_{C2}$ (Ctr) and present as mean ± s.e.m. from at least three independent biological replicates, each performed in triplicate. The indicated number of independent experiments (n): Ctr, R655$^{3.32}$A, R656$^{3.33}$A, K745^{ECL2}E, C746^{ECL2}A, I748^{ECL2}A, D750$^{5.37}$A, L753$^{5.40}$A, F805$^{6.57}$A: n = 9, 5, 4, 3, 4, 4, 4, 4, 4. **j**, Effect of VU0155041 (3.16 μM) alone on mGlu2-4 heterodimer or indicated mutants. Data are shown as mean ± s.e.m. from at least three independent biological replicates. For Ctr, R655$^{3.32}$A, R656$^{3.33}$A, K745^{ECL2}E, C746^{ECL2}A, I748^{ECL2}A, D750$^{5.37}$A, L753$^{5.40}$A, F805$^{6.57}$A respectively: n = 3, 5, 4, 3, 4, 4, 4, 4, 4. Data are analyzed using one-way ANOVA with a Dunnett's post-hoc multiple comparison test compared with Ctr to determine significance. ****P < 0.0001, *P < 0.05. **k**, Response of different concentration of VU0155041 with EC_{20} of Glutamate (0.8 μM) in mGlu2$_{C1}$-mGlu4$_{C2}$ heterodimer Ctrl and the indicated mutants. Data are normalized by using the maximum response (E_{max}) of VU0155041 in the cells transfected with mGlu2$_{C1}$ and mGlu4$_{C2}$ (Ctr) and present as mean ± s.e.m. from at least three

independent biological replicates, each performed in triplicate. For Ctr, R655$^{3.32}$A, R656$^{3.33}$A, K745^{ECL2}E, C746^{ECL2}A, I748^{ECL2}A, D750$^{5.37}$A, L753$^{5.40}$A, F805$^{6.57}$A respectively: n = 5, 5, 5, 4, 3, 4, 4, 4, 4. *P* values for *(k)*: <0.0001, <0.0001, <0.0001, <0.0001, <0.0001, 0.0225, <0.0001, <0.0001 (from left to right).

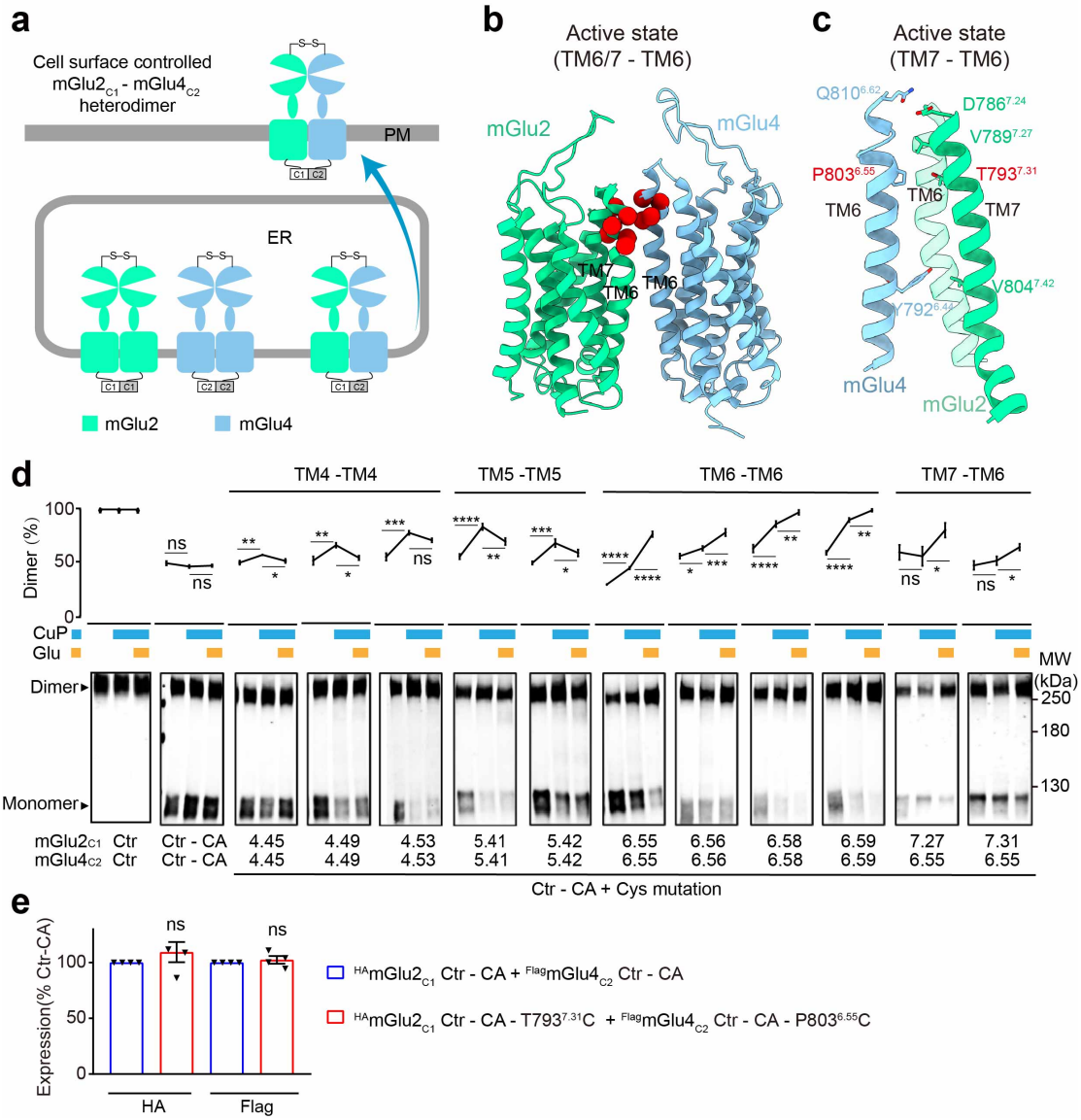

Supplementary Fig. 10. Interaction interface of the 7TMs. a, Cartoons showing the quality control system that allows only the controlled $mGlu2_{C1}$-$mGlu4_{C2}$ heterodimer to reach cell surface. PM, plasma membrane. **b**, Cysteine substitutions in the TM6 or TM7 of mGlu2 (position 6.55, 6.56, 6.58, 6.59, 7.27, 7.31) or mGlu4 (position 6.55, 6.56, 6.58, 6.59) subunit in crosslinking experiments are highlighted by a red ball (α carbon) in active state. **c,** Detail interaction between TM7 of mGlu2 and TM6 of mGlu4 subunit in the mGlu-2_G complex. **d**, Cross-linking of cell surface mGlu2 and mGlu4 subunits between the indicated residues mutated into cysteine (Cys), in the indicated TM helices, without or with CuP (blue) and with Glu (yellow). Ctr, $mGlu2_{C1}$-$mGlu4_{C2}$ heterodimer. Ctr-CA, Ctr with C121A mutation in mGlu2 and C136A-C715A mutation in mGlu4 to avoid disulfide bonds between mGlu4 subunits. Ctr-CA + Cys mutation, Ctr-CA with an additional single Cys mutation to alanine in the indicated TMs of mGlu2 or mGlu4. Data of the percentage of dimer in the three treatments (without CuP and Glu, with CuP, with CuP and Glu) of each mutation are mean ± s.e.m. from at least three independent biological replicates. The number of independent experiments (n) for Ctr and indicated receptors are n = 3, 16, 4, 5, 4, 6, 5, 7, 4, 6, 7, 5, 5. Data are analyzed using one-way ANOVA with a Dunnett's post-hoc multiple comparison test for each group of three treatments (no CuP/no Glu, CuP/no Glu, CuP and Glu), through comparing the mean of each treatment with the mean of every other treatment to determine significance. ****$P < 0.0001$, ***$P < 0.001$,

P < 0.01, *P < 0.05, not significant (ns) > 0.05. **e, Expression of mGlu2-4 Ctr-CA and Ctr-CA + T793$^{7.31}$C + P803$^{6.55}$C in Fig. 3d detected by HA or Flag antibodies. Data are normalized with mGlu2-4 Ctr-CA and present as mean ± s.e.m. from four independent biological replicates. Data are analyzed using unpaired student t test to determine significance. not significant (ns) > 0.05. P values for *(d)*: 0.0664, 0.7958, 0.0050, 0.0203, 0.0068, 0.0223, 0.0002, 0.1335, <0.0001, 0.0080, 0.0003, 0.0358, <0.0001, <0.0001, 0.0195, 0.0009, <0.0001, 0.0095, <0.0001, 0.0025, 0.7490, 0.0374, 0.7063, 0.0106 (from left to right).

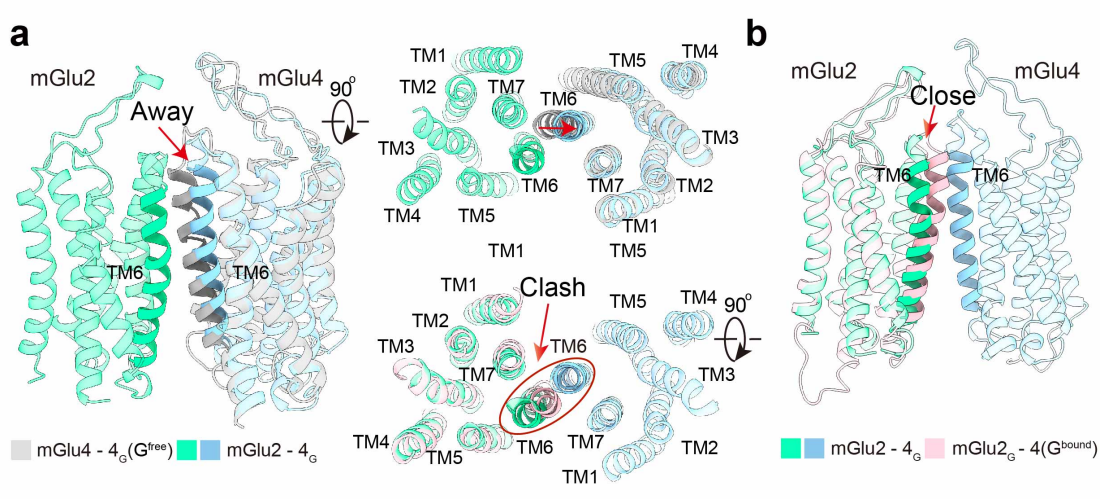

Supplementary Fig. 11. Inter-subunits allosteric regulation of the 7TMs. a, Side and extracellular views of the mGlu2-4_G 7TM interface in this study compared with that of the mGlu4-4_G complex (PDB: 8JD6). The upper end of TM6 of mGlu4 in mGlu2-4_G further moves away from mGlu2 compared with G^{free} mGlu4 (PDB: 8JD6), to avoid TM6-TM6 clash in mGlu2-4_G. **b**, Side and extracellular views of the mGlu2-4_G 7TM interface in this study where the mGlu2 subunit was superimposed with the mGlu2 subunit with G protein bound from the $mGlu2_G$-4 complex (PDB: 8JD5). The close proximity of the two TM6 domains creates a potential steric hindrance, impeding the formation of the proper TM6-TM6 interface necessary for G protein activation.

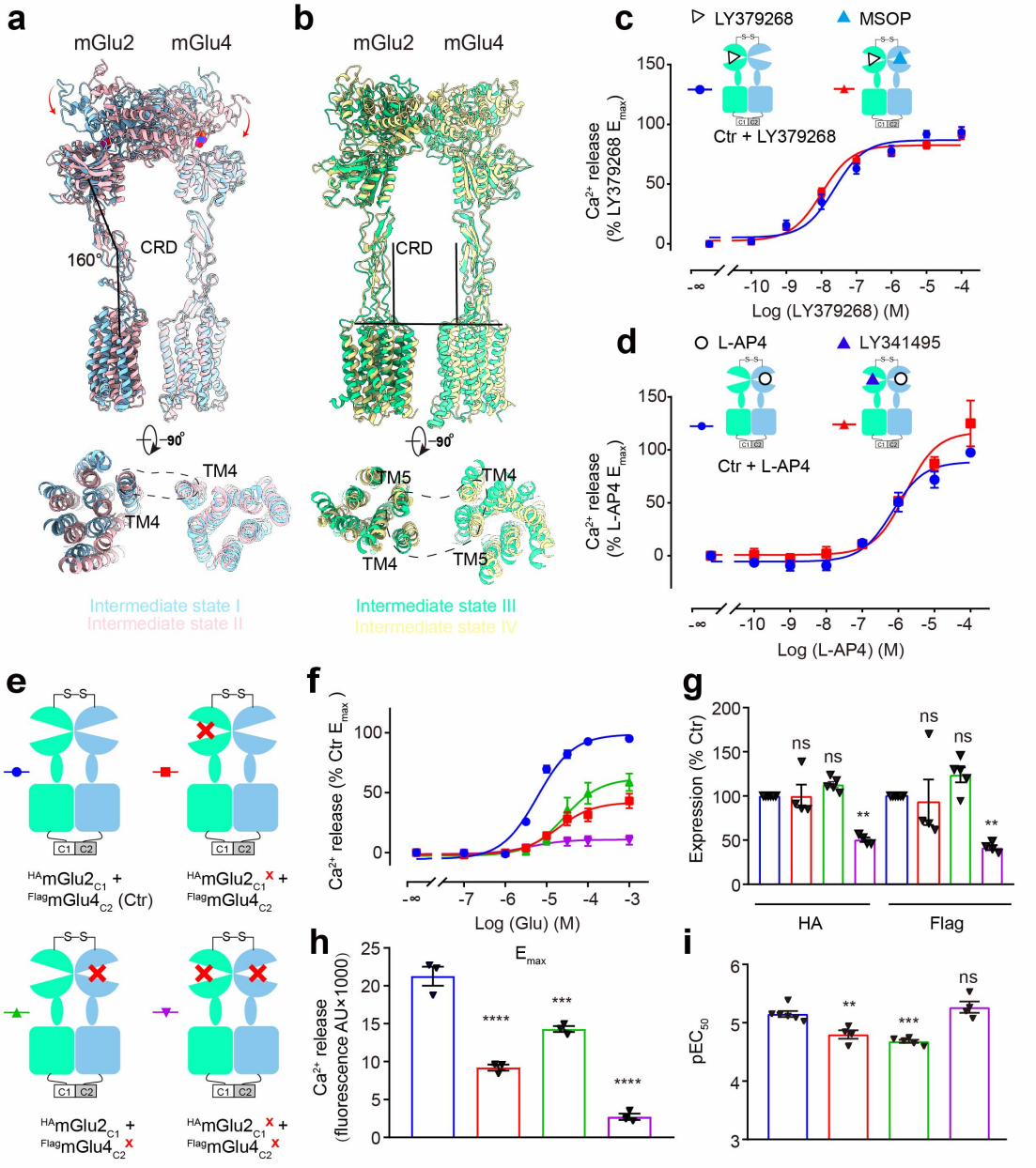

Supplementary Fig. 12. Intermediate state for mGlu2-4 heterodimer and CRD interaction. a-b, Superimposed structures of two different indicated intermediate states with *(a)* or without *(b)* mGlu2 CRD bending. **c**, Ca^{2+} responses induced by mGlu2 agonist LY379268 with or without mGlu4 antagonist MSOP in $mGlu2_{C1}$-$mGlu4_{C2}$ receptor. **d**, Ca^{2+} responses induced by mGlu4 agonist L-AP4 with or without mGlu2 antagonist LY341495 in $mGlu2_{C1}$-$mGlu4_{C2}$ receptor. Data in *(c)* and *(d)* are normalized accordingly and present as mean ± s.e.m. from at least three independent biological replicates, each performed in triplicate. The indicated number of independent experiments for *(c)*, LY379268, LY379268 + MSOP: n = 5, 5; *(d)*, L-AP4, L-AP4 + LY341495: n = 3, 3. **e,** Schemes of the constructs used in *(f-i)*: $mGlu2_{C1}$-$mGlu4_{C2}$ heterodimer (Ctr); Ctr with the mutation SATA in mGlu2 or mGlu4 binding pocket (red crosses), which blocks the agonist binding. **f**, Glu-induced Ca^{2+} release in $mGlu2_{C1}$-$mGlu4_{C2}$ heterodimer (Ctr) with or without the mutation SATA in mGlu2 or mGlu4 binding pocket. Data are normalized with the E_{max} of Ctr, and present as mean ± s.e.m. from at least three independent biological replicates. For Ctr, $mGlu2_{C1}{}^{x}$ + $mGlu4_{C2}$, $mGlu2_{C1}$ + $mGlu4_{C2}{}^{x}$, $mGlu2_{C1}{}^{x}$ + $mGlu4_{C2}{}^{x}$ respectively, n = 6, 5, 4, 6. **g**, Expression of receptors

in *(f)* detected by HA or Flag antibodies. **h**, Representative E_{max} of Ca^{2+} release in *(f)*. **i**, pEC_{50} of Glu in *(f)*. Data in *(g-i)* are present as mean ± s.e.m. and analyzed using one-way ANOVA with a Dunnett's post-hoc multiple comparison test compared with Ctr to determine significance. ****$P < 0.0001$, ***$P < 0.001$, **$P < 0.01$, *$P < 0.05$, not significant (ns) > 0.05. *P* values for *(g)*: >0.9999, 0.9572, 0.0117, 0.9991, 0.5050, 0.0018 (from left to right). *P* values for *(h)*: <0.0001, 0.0004, 0.0001; *(i)*: 0.0027, 0.0001, 0.4236 (from left to right).

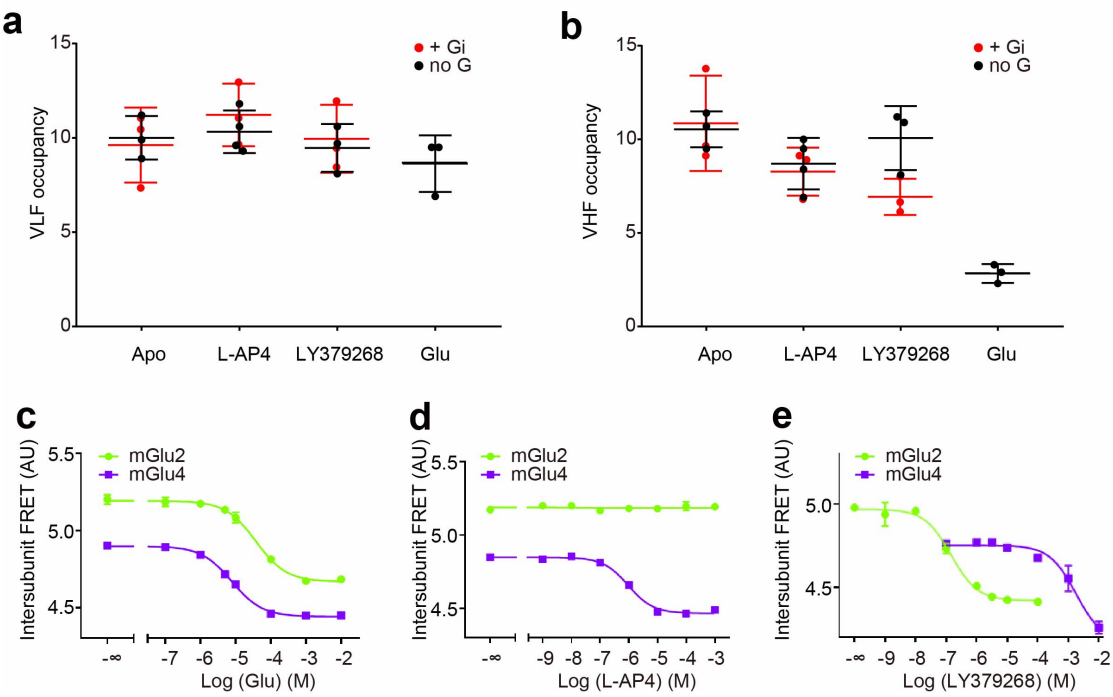

Supplementary Fig. 13. Population of additional FRET states and dose-dependent VFT reorientation of mGlu2 and mGlu4 homodimers. a-b, Fraction of molecules in the very low FRET (VLF, *a*) and very high FRET (VHF, *b*) states in the absence (black) or presence of heterotrimeric Gi complex (red). Shown are the mean ± SD of at least three independent biological replicates obtained from the number of molecules found in the VLH or VHF populations of histograms shown in Fig. 4c-d of the main text (white gaussians) over the sum of all molecules. **c-e**, Ligand-dependent VFT reorientation of detergent solubilized mGlu2 and mGlu4 homodimers, N-terminally SNAP-labelled with Lumi4-Tb and green SNAP substrates, upon titration with the natural full agonist glutamate *(c)*, group III specific agonist L-AP4 *(d)* and group II agonist LY379268 *(e)*. Data are mean ± s.e.m. of triplicates from a representative experiment.

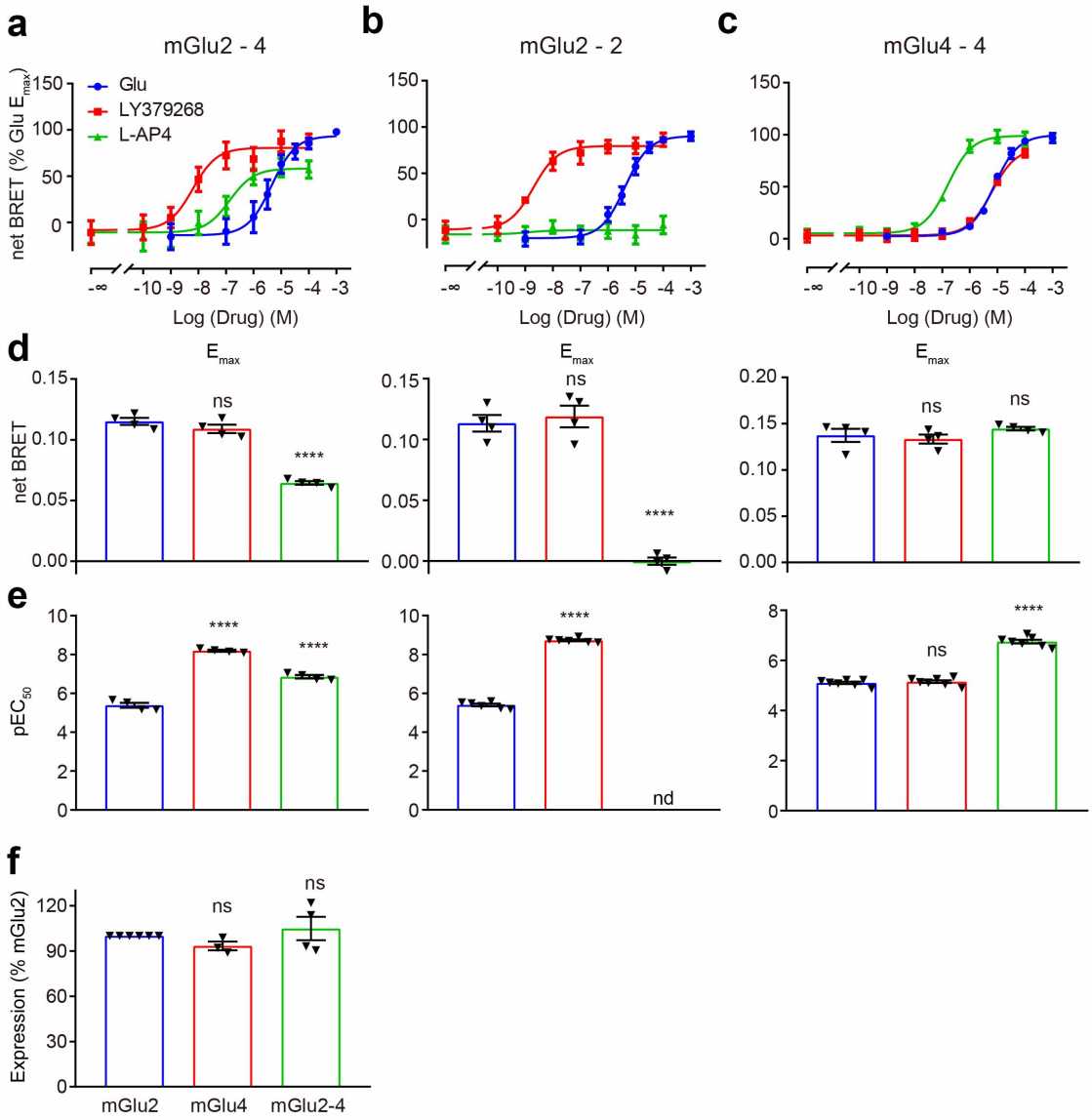

Supplementary Fig. 14. Glu, LY379268 and L-AP4-induced mGlu2-4 heterodimer, mGlu2-2 homodimer and mGlu4-4 homodimer activation. a-c, Dose response curves of Glu, LY379268 and L-AP4 in mGlu2-4 *(a)*, mGlu2-2 *(b)* and mGlu4-4 *(c)*. Data are normalized with the E_{max} of Glu and present as mean ± s.e.m. from at least three independent biological replicates. The indicated number of independent experiments for Glu, LY379268, L-AP4 respectively, in *(a)*: n = 4, 4, 4; in *(b)*: n = 6, 5, 5; in *(c)*: n = 7, 6, 7. **d**, Representative E_{max} of mGlu2-4 heterodimer, mGlu2-2 homodimer and mGlu4-4 homodimer activated by Glu, LY379268 and L-AP4 in *(a-c)*. **e**, pEC_{50} of Glu, LY379268 and L-AP4 in *(a-c)*. **f**, Expression of mGlu2-4 heterodimer, mGlu2-2 homodimer and mGlu4-4 homodimer in *(a-c)*. Data in *(d-f)* are present as mean ± s.e.m and analyzed using one-way ANOVA with a Dunnett's post-hoc multiple comparison test compared with Glu in *(d-e)* or mGlu2 in *(f)* to determine significance. ****P < 0.0001, not significant (ns) > 0.05. nd, not determined (data for which a robust concentration response curve or plateau could not be established within the concentration range tested). P values for *(d)*: 0.2428, <0.0001, 0.7872, <0.0001, 0.7986, 0.5221; *(e)*: <0.0001, <0.0001, 0.0001, 0.7995, <0.0001; *(f)*: 0.4939, 0.6251 (from left to right).

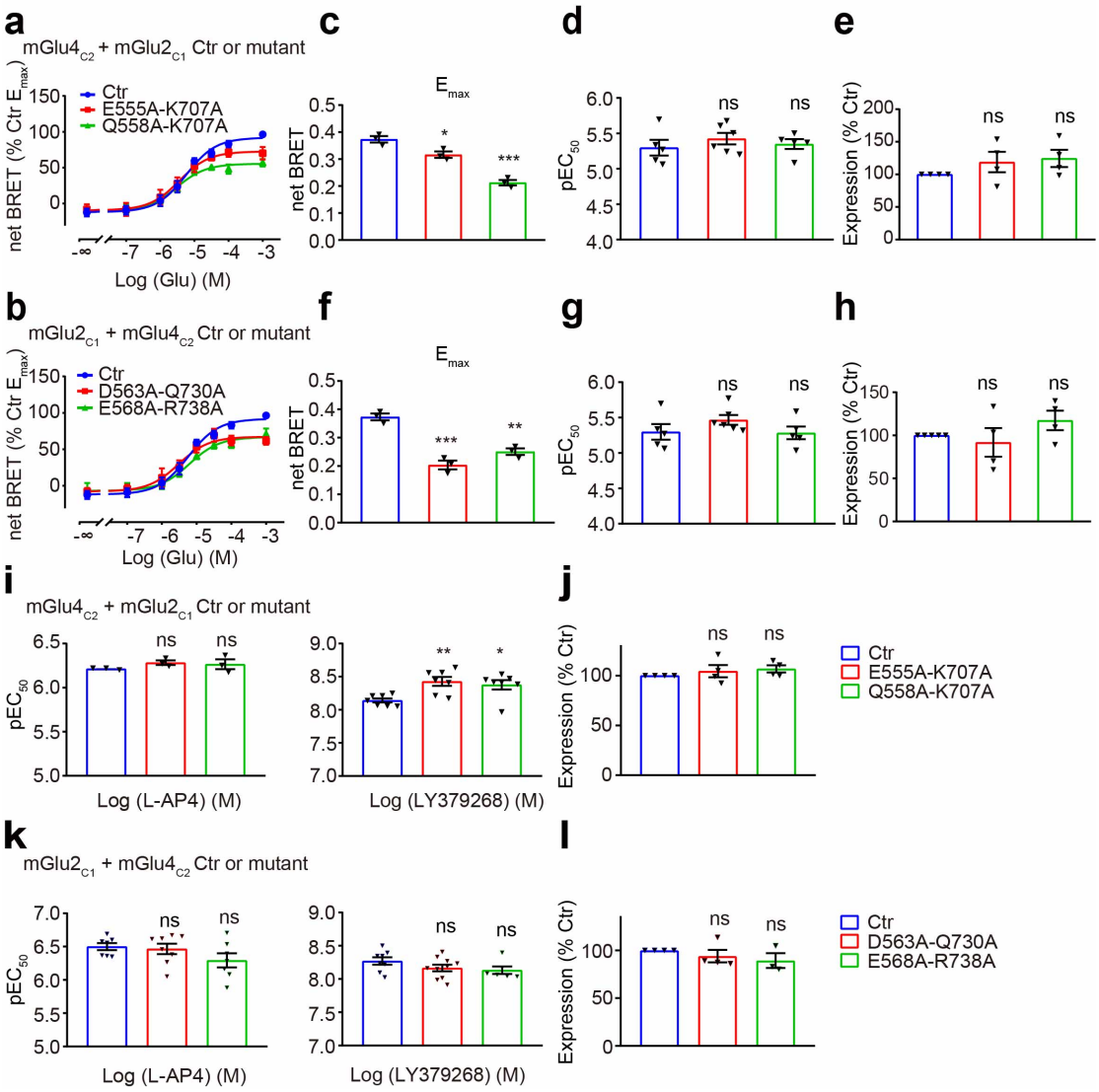

Supplementary Fig. 15. Intermediate state for mGlu2-4 heterodimer and CRD interaction. a-b, Glu-induced G protein activation in mGlu2$_{C1}$-mGlu4$_{C2}$ heterodimer (Ctr), without or with the indicated mutations in the CRD and ECL2 of mGlu2 subunit *(a)* or mGlu4 subunit *(b)*. Data are normalized with the E_{max} of Ctr and present as mean ± s.e.m. from at least three independent biological replicates. The indicated number of independent experiments in *(a)*, for Ctr, E555A-K707A, Q558A-K707A respectively, n = 4, 3, 4; *(b)*, Ctr, E568A-R738A, D563A-Q730A, n = 7, 4, 5. **c**, Representative E_{max} of mGlu2$_{C1}$-mGlu4$_{C2}$ and the mutants in *(a)*. **d-e**, pEC_{50} and expression of mGlu2$_{C1}$-mGlu4$_{C2}$ and the mutants in *(a)*. **f**, Representative E_{max} of mGlu2$_{C1}$-mGlu4$_{C2}$ and the mutants in *(b)*. **g-h**, pEC_{50} and expression of mGlu2$_{C1}$-mGlu4$_{C2}$ and the mutants in *(b)*. **i-l**, pEC_{50} and expression of mGlu2$_{C1}$-mGlu4$_{C2}$ and the indicated mutants in Fig. 5b-c. Data in *(c-f)* are present as mean ± s.e.m. and analyzed using one-way ANOVA with a Dunnett's post-hoc multiple comparison test compared with Ctr to determine significance. ***$P < 0.001$, **$P < 0.01$, *$P < 0.05$, not significant (ns) > 0.05. P values for *(c)*: 0.0211, 0.0001. P values for *(d)*: 0.5031, 0.8960. P values for *(e)*: 0.4506, 0.2917. P values for *(f)*: 0.0002, 0.0010; *(g)*: 0.3256, 0.9910; *(h)*: 0.8109, 0.4342; *(i)*: 0.3531, 0.5371, 0.0057, 0.0210; *(j)*: 0.6682, 0.4332; *(k)*: 0.9342, 0.1649, 0.2735, 0.1885; *(l)*: 0.6429, 0.3507 (all from left to right).

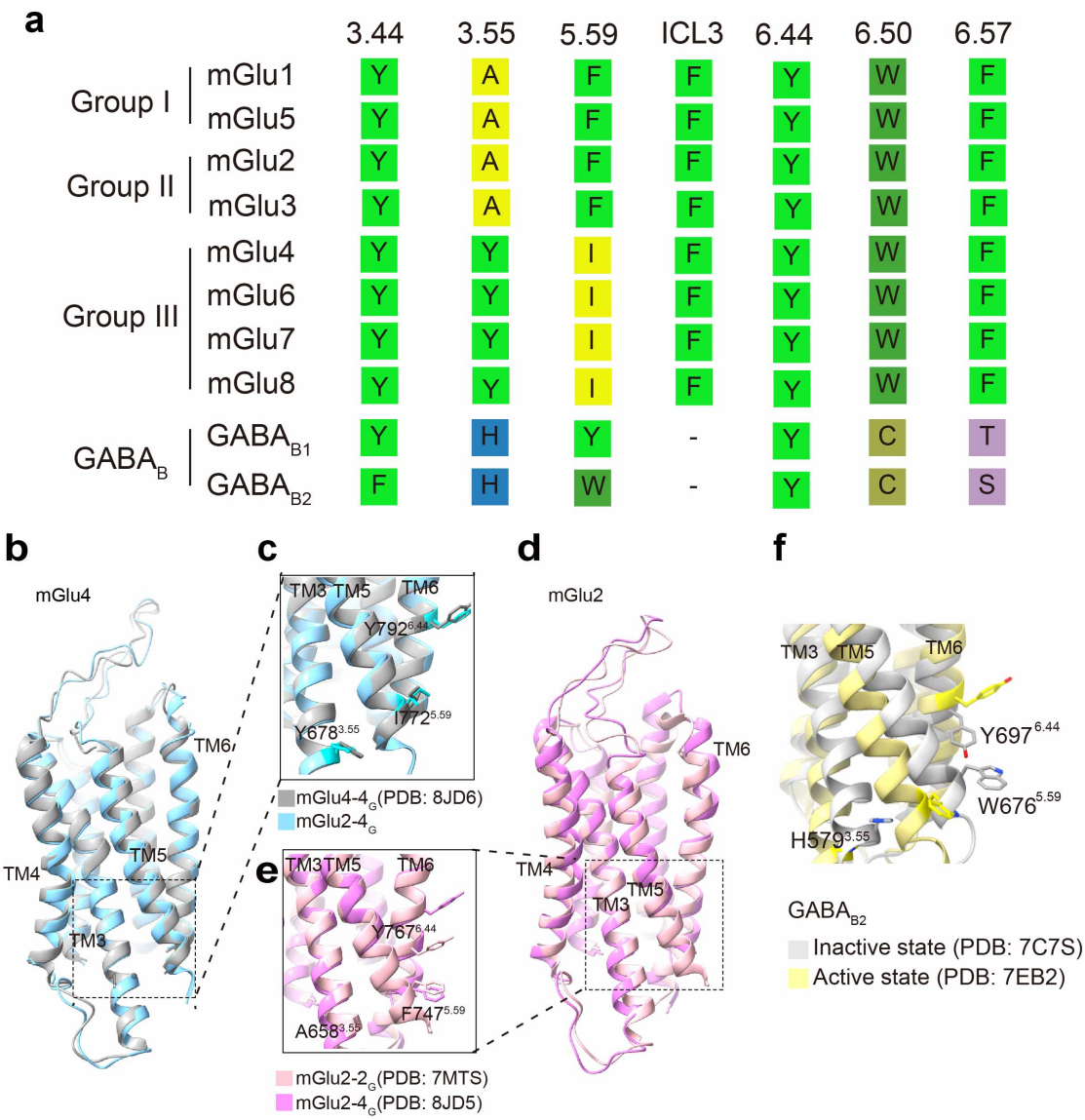

Supplementary Fig. 16. Intra-subunit conformational changes of the 7TM within mGlu2-4 heterodimer. a, Sequence alignment of the critical residues among the indicated mGlu and $GABA_B$ receptors. In ICL3, the indicated F is in the motif FNEAK, which is highly conserved in all the mGlu receptors. **b-c,** Side view *(b)* and magnified view *(c)* of conformational changes of 7TM between mGlu4 subunit in mGlu2-4_G complex compared with mGlu4-4_G complex (PDB: 8JD6). **d-e**, Side view *(d)* and magnified view *(e)* of conformational changes of 7TM between mGlu2 subunit in mGlu2-2_G (PDB: 7MTS) complex compared with mGlu2_G-4 complex. **f**, Magnified view of conformational changes of $GABA_{B2}$ upon activation.

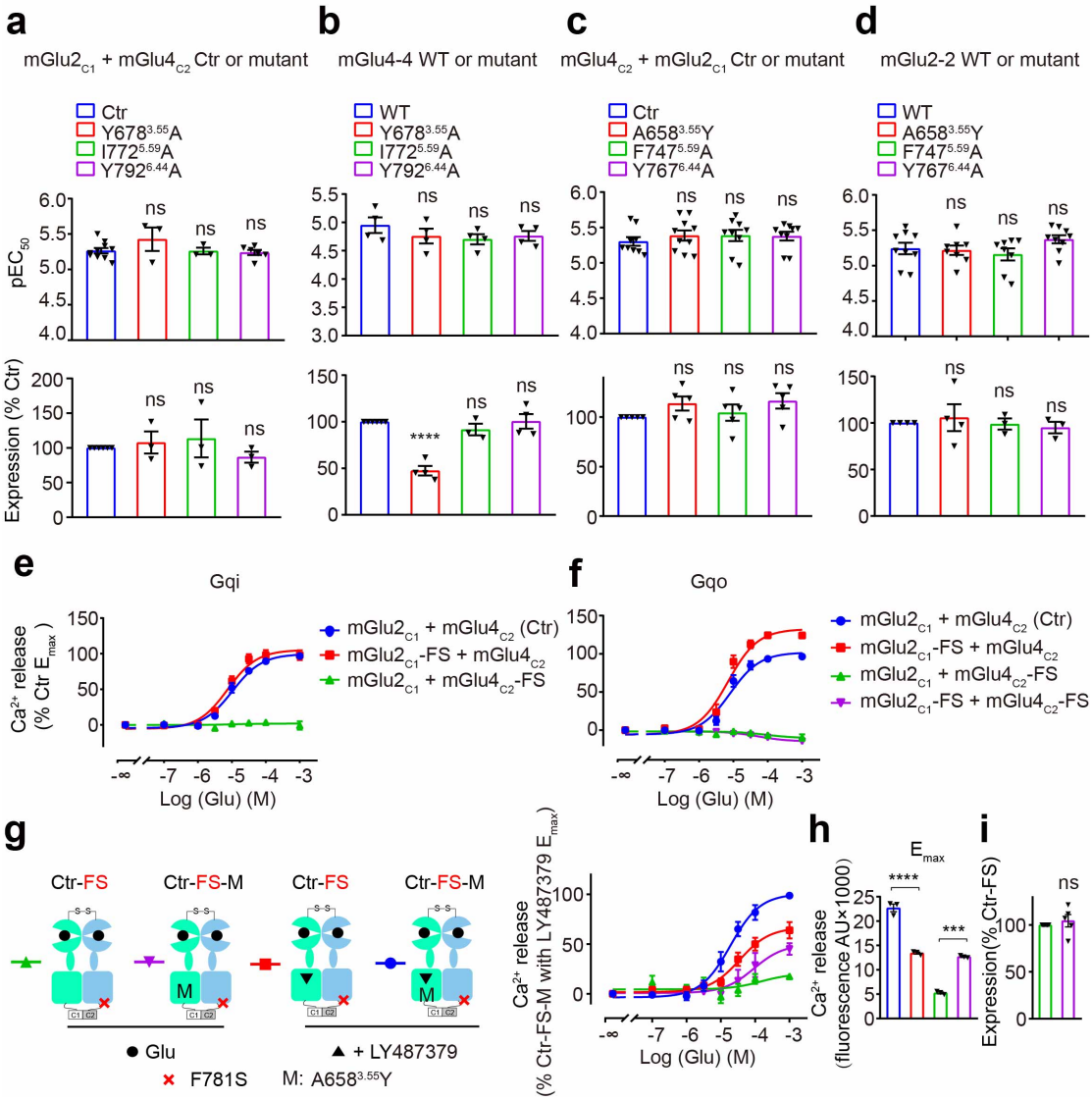

Supplementary Fig. 17. TM3-5-6 network conformational changes of mGlu2-4 heterodimer. a-d, pEC_{50} and expression of $mGlu2_{C1}$-$mGlu4_{C2}$ heterodimer (Ctr), mGlu2-2 (WT) or mGlu4-4 homodimer (WT), and the indicated mutants in Fig. 6c-d. **e-f**, Glu induced Ca^{2+} release in $mGlu2_{C1}$-$mGlu4_{C2}$ heterodimer (Ctr) with or without the mutation FS in mGlu2 or mGlu4 co-transfected with chimeric G protein G_{qi9} *(e)* or G_{qo} *(f)*. Data are normalized with the E_{max} of Ctr and present as mean ± s.e.m. from at least three independent biological replicates. The indicated number of independent experiments in *(e)*, for $mGlu2_{C1}$ + $mGlu4_{C2}$ heterodimer (Ctr), $mGlu2_{C1}$-FS + $mGlu4_{C2}$ and $mGlu2_{C1}$ + $mGlu4_{C2}$-FS respectively, n = 9, 4, 5; in *(f)*, for $mGlu2_{C1}$ + $mGlu4_{C2}$ heterodimer (Ctr), $mGlu2_{C1}$-FS + $mGlu4_{C2}$, $mGlu2_{C1}$ + $mGlu4_{C2}$-FS and $mGlu2_{C1}$-FS + $mGlu4_{C2}$-FS respectively, n = 4, 4, 4, 4. **g**, Glu-induced Ca^{2+} release in the presence or absence of LY487379 (20 μM) in $mGlu2_{C1}$-$mGlu4_{C2}$ heterodimer with F781S mutation in mGlu4 subunit (Ctr-FS), or Ctr-FS with an additional mutation $A658^{3.55}Y$ (M) in mGlu2 subunit (Ctr-FS-M) that may create clashes with TM5 in mGlu2, which then favors the active state of mGlu2 7TM. Data are normalized with the E_{max} of Ctr-FS-M with LY487379 and present as mean ± s.e.m. from at least three independent experiments. For Ctr-FS, Ctr-FS-M, Ctr-FS + LY487379, Ctr-FS-M + LY487379 respectively, n = 5, 4, 6, 7. **h**, Representative E_{max} of Glu response in *(g)*. **i**, Expression of receptors in *(g)*. Data are present as mean ± s.e.m. in *(a-d)* and *(h-i)*. Data in *(a-d)* are analyzed using one-way ANOVA with a Dunnett's post-hoc multiple comparison test compared with Ctr or WT to determine significance. Data in *(i)*

are analyzed using unpaired student t test to determine significance. ****$P < 0.0001$, ***$P < 0.001$, not significant (ns) > 0.05. *P* values for *(a)* upper: 0.2389, >0.9999, 0.9779; lower: 0.9482, 0.7915, 0.8015; *(b)* upper: 0.5117, 0.3241, 0.5242; lower: <0.0001, 0.5315, 0.9997; *(c)* upper: 0.7219, 0.7294, 0.7902; lower: 0.3642, 0.9324, 0.2399; *(d)* upper: 0.9917, 0.7654, 0.4442; lower: 0.9408, 0.9994, 0.9644 (all from left to right).

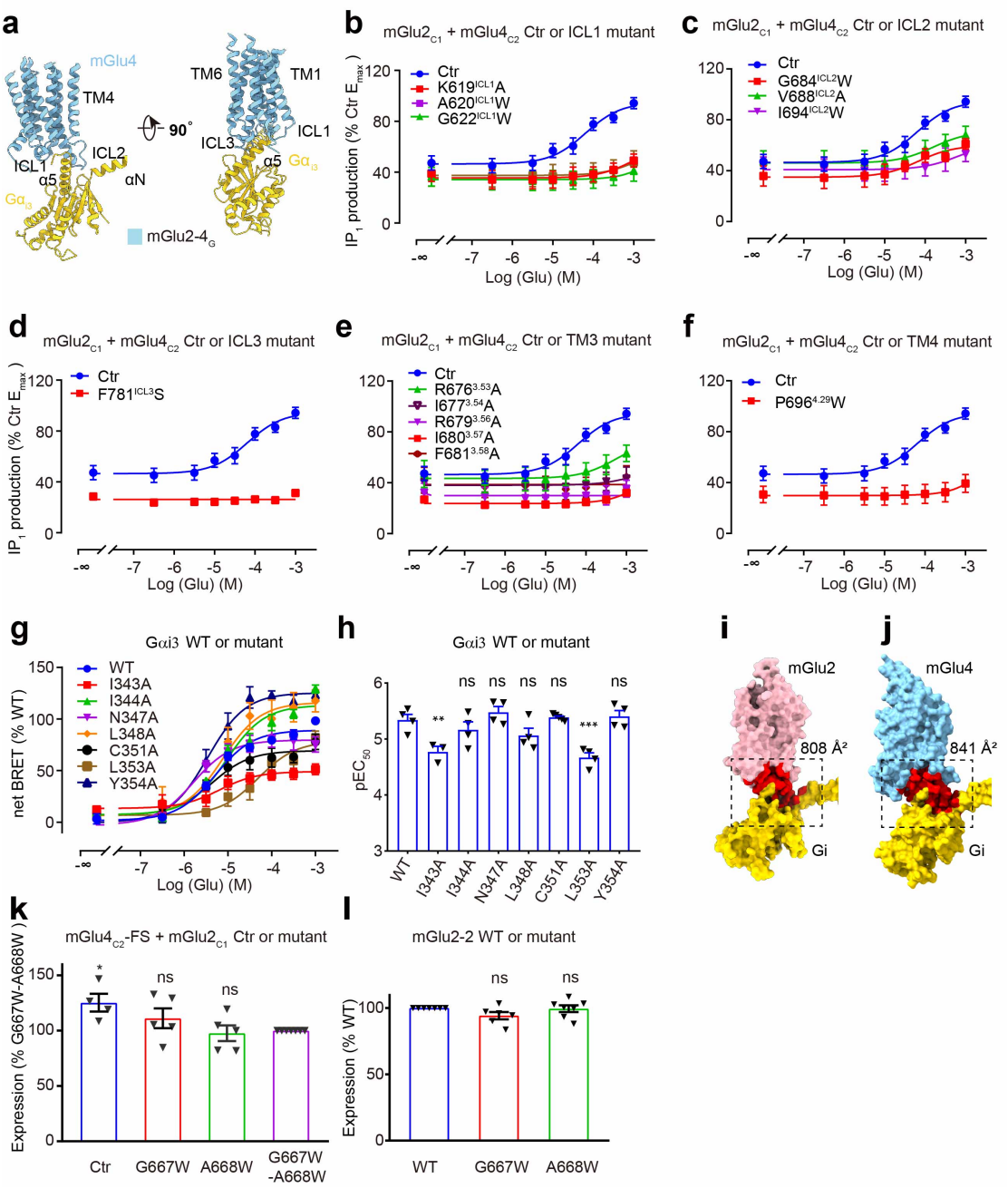

Supplementary Fig. 18. The G_i protein binding pocket in mGlu4 subunit of mGlu2-4 heterodimer. a, The G_i binding pocket in mGlu2-4_G complex, which was formed by the intracellular ends of TM3 and three ICLs of mGlu4 subunit. **b-f**, Dose response curves of Glu-induced IP_1 production in mGlu2_{C1}-mGlu4_{C2} heterodimer (Ctr) with or without indicated mutations in mGlu4 subunit. Data are normalized with the E_{max} of Ctr and present as mean ± s.e.m. from at least three independent experiments. For Ctr, $K619^{ICL1}A$, $A620^{ICL1}W$, $G622^{ICL1}W$, $G684^{ICL2}W$, $V688^{ICL2}A$, $I694^{ICL2}W$, $F781^{ICL3}S$, $R676^{3.53}A$, $I677^{3.54}A$, $R679^{3.56}A$, $I680^{3.57}A$, $F681^{3.58}A$, $P696^{4.25}W$ respectively, n = 10, 4, 5, 5, 3, 4, 4, 3, 4, 5, 4, 3, 5, 3. **g**, G protein rearrangement induced by Glu on Nluc-tagged $G\alpha_{i3}$ WT or the indicated mutants, which involve mutation of C-terminal residues of $G\alpha_{i3}$ having direct interaction with mGlu4 subunit. Data are normalized with the E_{max} of WT and present as mean ± s.e.m. from at least three independent experiments. For WT, I343A, I344A, N347A, L348A, C351A, L353A, Y354A respectively, n = 5, 5, 3, 3, 3, 4, 3, 3. **h**, pEC_{50} of G protein signaling on mGlu2-4 heterodimer with Nluc-tagged $G\alpha_{i3}$ WT or the indicated mutants in *(g)*. Data are

analyzed using one-way ANOVA with a Dunnett's post-hoc multiple comparison test compared with WT to determine significance. **i-j**, Interface area of $mGlu2_G$-4 and G_i protein (PDB: 8JD5) *(i)* or mGlu2-4_G and G_i protein *(j)*. The interaction interface between the receptor and G_i is colored red. **k-l,** Expression of the receptors in Fig. 8b and 8d. Data are present as mean ± s.e.m. from at least three independent experiments and analyzed using one-way ANOVA with a Dunnett's post-hoc multiple comparison test compared with Ctr or WT to determine significance. ***$P < 0.001$, **$P < 0.01$, *$P < 0.05$, not significant (ns) > 0.05. P values for *(h)*: 0.0065, 0.7152, 0.8705, 0.2681, 0.9994, 0.0006, 0.9971; *(k)*: 0.0295, 0.4307, 0.9866; *(l)*: 0.1242, 0.9743 (all from left to right).

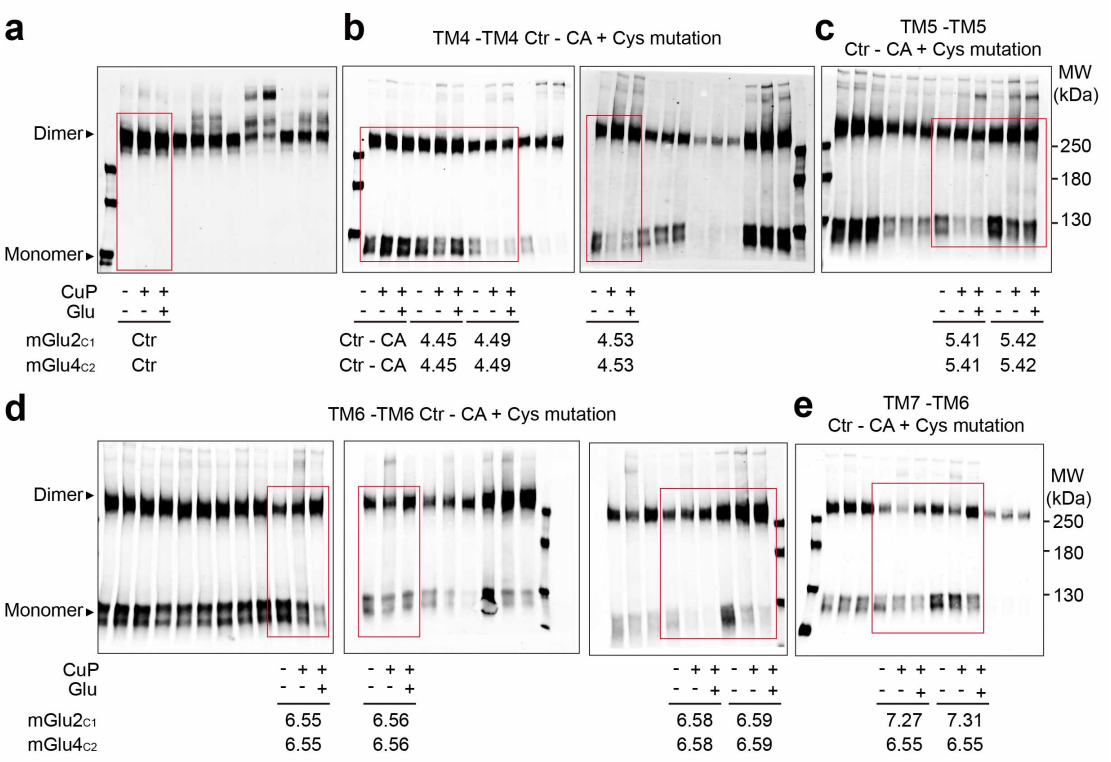

Supplementary Fig. 19. Uncropped gels and blots corresponding to the Supplementary Fig. 10. Cropped regions are indicated as red boxes. **a-e**, Uncropped gel image for Supplementary Fig. 10d. Ctr, $mGlu2_{C1}$-$mGlu4_{C2}$ heterodimer. Ctr-CA, Ctr with C121A mutation in mGlu2 and C136A-C715A mutation in mGlu4 to avoid disulfide bonds between mGlu4 subunits. Ctr-CA + Cys mutation, Ctr-CA with an additional single Cys mutation to alanine in the indicated TMs of mGlu2 or mGlu4.

Supplementary Table 1. Cryo-EM data collection, model refinement, and validation statistics.

	Glu-VU0155041-mGlu2-4-Gi	LY341495-CPPG-mGlu2-4	L-AP4-mGlu2-4	LY379268-mGlu2-4
Data collection and processing				
Magnification	150538	150538	150538	150538
Voltage (kV)	300	300	300	300
Electron exposure ($e^-/Å^2$)	52	52	52	52
Defocus range (μm)	0.7 to 1.5	0.7 to 1.5	0.7 to 1.5	0.7 to 1.5
Pixel size (Å)	0.93	0.93	0.93	0.93
Symmetry imposed	C1	C1	C1	C1
Initial particle projections (no.)	24,683,667	20,724,986	14,038,794	12,952,064
Final particle projections (no.)	157,293	94,971	112,924	106,936
Map resolution (Å)	3.7	4.45	4.46	5.95
FSC threshold	0.143	0.143	0.143	0.143
Map resolution range (Å)	3.7-4.9	4.0-9.0	3.8-8.6	4.0-9.0
Refinement				
Initial model used (PDB code)	7E9G	Alpha Fold2	Alpha Fold2	Alpha Fold2
Model Resolution (Å)	4.0	7.1	7.4	7.4
FSC threshold	0.5	0.5	0.5	0.5
Map sharpening method	DeepEMhancer	Cryosparc	Cryosparc	Cryosparc
Model Composition				
Non-hydrogen atoms	16799	6077	6057	6193
Protein residues	2145	1508	1511	1545
Ligand	3	2	1	1
B factors ($Å^2$)				
Protein	30-119.61	19.07-79.42	13.83-75.76	30.00-110.30
Ligand	20.00	20.00	20.00	20.00
RMSD				
Bound lengths (Å)	0.005	0.011	0.011	0.012
Bound angles (°)	1.168	2.099	2.040	2.137
Validation				
MolProbity score	2.09	1.11	1.24	1.06
Clash score	14.29	1.04	1.30	0.76
Rotamer outliers (%)	0	0	0	0
Ramachandran Plot				
Favored (%)	93.53	95.37	94.31	95.49
Allowed (%)	6.47	4.43	5.69	4.51
Disallowed (%)	0	0	0	0
EMDB accession number	EMD-37507	EMD-37509	EMD-37506	EMD-37508
PDB accession number	8WGB	8WGD	8WG9	8WGC

EMDB, Electron Microscopy Data Bank; FSC, Fourier correlation;
PDB, Protein Data Bank; RMSD, root-mean-square deviation.

Supplementary Table 2. Mean FRET efficiencies for the four populations identified determined in the absence of ligand (Apo) or in the presence of ligands.

	mean E Apo	sigma Apo	mean E ligands	sigma ligands
VLF	0.02	0.09	0.02	0.09
LF	0.28	0.10	0.28	0.10
HF	0.54	0.11	0.50	0.11
VHF	0.88	0.11	0.88	0.11

Supplementary Table 3. Proportion of each FRET populations for the mGlu2-4 heterodimer under the indicated conditions. Values are means ± S.D. of three biological replicates.

	Apo	Apo + Gi	L-AP4	L-AP4 + Gi	LY 379268	LY 379268 + Gi	Glutamate
VLF	10.0 ± 0.9	9.6 ± 1.6	10.3 ± 1.0	11.2 ± 1.3	9.5 ± 1.0	9.9 ± 1.5	8.6 ± 1.2
LF	10.6 ± 2.4	14.6 ± 2.3	21.0 ± 2.3	37.5 ± 2.9	27.0 ± 0.6	44.1 ± 0.2	77.8 ± 0.6
HF	68.9 ± 0.9	62.3 ± 3.3	60.0 ± 2.0	41.3 ± 2.3	56.6 ± 1.2	37.8± 1.8	10.7 ± 0.8
VHF	10.5 ± 0.8	13.5 ± 2.8	8.7 ± 1.2	10.1 ± 1.4	6.9 ± 0.5	8.3 ± 1.1	2.8 ± 0.4

Supplementary Table 4. IP_1 production, Gi activation and Ca^{2+} release of mGlu 2-4 receptor and indicated mutants.

	L-AP4-induced G protein activation					LY379268-induced G protein activation					
	EC_{50} (μM)	EC_{50} ratio	pEC_{50} (mean ± s.e.m.)	E_{max} (% Ctr)	n	EC_{50} (nM)	EC_{50} ratio	pEC_{50} (mean ± s.e.m.)	E_{max} (% Ctr)	n	Expression (% Ctr)
$mGlu2_{C1}$-Ctr + $mGlu4_{C2}$	0.6	1.0	6.21 ± 0.01	100	3	7.2	1.0	8.14 ± 0.03	100	5	100
$mGlu2_{C1}$-E555A-K707A + $mGlu4_{C2}$	0.5	0.9	6.28 ± 0.05	77 ± 3	3	3.7	0.5	8.43 ± 0.07	55 ± 5	5	105 ± 6
$mGlu2_{C1}$-Q558A-K707A + $mGlu4_{C2}$	0.5	0.9	6.27 ± 0.06	82 ± 2	3	4.2	0.6	8.38 ± 0.07	60 ± 7	4	107 ± 4
$mGlu4_{C2}$-Ctr + $mGlu2_{C1}$	0.3	1.0	6.56 ± 0.08	100	7	5.2	1.0	8.28 ± 0.11	100	8	100
$mGlu4_{C2}$-D563A-Q730A + $mGlu2_{C1}$	0.3	1.2	6.47 ± 0.08	73 ± 4	5	6.8	1.3	8.17 ± 0.05	137 ± 7	4	94 ± 7
$mGlu4_{C2}$-E568A-R738A + $mGlu2_{C1}$	0.6	2.2	6.22 ± 0.12	40 ± 6	5	8.9	1.7	8.05 ± 0.07	98 ± 8	5	89 ± 8

Glu-induced G protein activation						
$mGlu2_{C1}$(Ctr or mutant) + $mGlu4_{C2}$ (Ctr or mutant)	EC_{50} (μM)	EC_{50} ratio	pEC_{50} (mean ± s.e.m.)	E_{max} (% Ctr)	n	Expression (% Ctr)
$mGlu2_{C1}$-Ctr + $mGlu4_{C2}$	5.8	1.0	5.24 ± 0.11	100	4	100
$mGlu2_{C1}$-E555A-K707A+ $mGlu4_{C2}$	3.7	0.6	5.43 ± 0.08	74 ± 8	3	119 ± 15
$mGlu2_{C1}$-Q558A-K707A+ $mGlu4_{C2}$	3.7	0.6	5.43 ± 0.10	60 ± 6	4	125 ± 13
$mGlu4_{C2}$-Ctr + $mGlu2_{C1}$	5.8	1.0	5.24 ± 0.11	100	7	100
$mGlu4_{C2}$-D563A-Q730A + $mGlu2_{C1}$	3.4	0.6	5.47 ± 0.07	67 ± 6	4	92 ± 17
$mGlu4_{C2}$-E568A-R738A + $mGlu2_{C1}$	6.2	1.1	5.21 ± 0.11	74 ± 9	5	127 ± 9

Gi activation of $mGlu2_{C1}$-$mGlu4_{C2}$ heterodimer (Ctr), mGlu4-4 homodimer (WT) or indicated mutants							
	Ctr, WT or mutant	EC_{50} (μM)	EC_{50} ratio	pEC_{50} (mean ± s.e.m.)	E_{max} (% Ctr or WT)	n	Expression (% Ctr or WT)
$mGlu2_{C1}$ + $mGlu4_{C2}$ Ctr or mutant	Ctr	5.5	1.0	5.26 ± 0.05	100	11	100
	Y678A	3.7	0.7	5.43 ± 0.17	50 ± 7	5	108 ± 16
	I772A	5.5	1.0	5.26 ± 0.05	126 ± 5	3	114 ± 27
	Y792A	5.9	1.1	5.23 ± 0.04	65 ± 8	4	87 ± 8
mGlu4-4 WT or mutant	WT	11.2	1.0	4.95 ± 0.14	100	4	100
	Y678A	17.4	1.5	4.76 ± 0.13	29 ± 6	4	47 ± 5
	I772A	19.5	1.7	4.71 ± 0.10	86 ± 4	3	92 ± 6
	Y792A	17.8	1.6	4.75 ± 0.08	32 ± 5	4	100 ± 8

Gi activation of $mGlu2_{C1}$-$mGlu4_{C2}$ heterodimer (Ctr), mGlu2-2 (WT) or with the mutations							
	Ctr, WT or mutant	**EC_{50} (μM)**	**EC_{50} ratio**	**pEC_{50} (mean ± s.e.m.)**	**E_{max} (% Ctr or WT)**	**n**	**Expression (% Ctr or WT)**
$mGlu4_{C2}$ + $mGlu2_{C1}$ Ctr or mutant	Ctr	5.0	1.0	5.30 ± 0.06	100	7	100
	A658Y	4.1	0.8	5.39 ± 0.07	109 ± 11	4	114 ± 7
	Y767A	4.1	0.8	5.39 ± 0.08	111 ± 6	4	119 ± 7
	F747A	4.9	1.0	5.31 ± 0.09	96 ± 7	5	105 ± 8
mGlu2-2 WT or mutant	WT	5.8	1.0	5.24 ± 0.08	100	9	100
	A658Y	6.0	1.0	5.22 ± 0.07	223 ± 10	7	106 ± 14
	Y767A	6.9	1.2	5.16 ± 0.09	166 ± 15	6	95 ± 6
	F747A	4.3	0.7	5.37 ± 0.06	186 ± 8	4	99 ± 6

Ca^{2+} release in $mGlu2_{C1}$-$mGlu4_{C2}$-FS heterodimer or with the mutations in mGlu2 ICL2							
	Ctr or mutant	**EC_{50} (μM)**	**EC_{50} ratio**	**pEC_{50} (mean ± s.e.m.)**	**E_{max} (% G667W-A668W)**	**n**	**Expression (% G667W-A668W)**
$mGlu4_{C2}$-FS + $mGlu2_{C1}$ Ctr or mutant	G667W-A668W	6.9	1.0	5.16 ± 0.05	100	7	100
	G667W	20.9	3.0	4.68 ± 0.07	41 ± 5	6	111 ± 9
	A668W	12.3	1.8	4.91 ± 0.07	75 ± 3	5	98 ± 7
	Ctr	7.1	1.0	5.15 ± 0.13	8 ± 1	6	125 ± 8

Ca^{2+} release in mGlu2-2 homodimer or with the mutations in ICL2							
	Ctr or mutant	**EC_{50} (μM)**	**EC_{50} ratio**	**pEC_{50} (mean ± s.e.m.)**	**E_{max} (% WT)**	**n**	**Expression (% WT)**
mGlu2-2 WT or mutant	WT	8.7	1.0	5.06 ± 0.05	100	8	100
	G667W	1.4	0.2	5.84 ± 0.08	103 ± 9	6	93 ± 3
	A668W	1.3	0.2	5.88 ± 0.07	112 ± 8	6	100 ± 3

Gi activation of $mGlu2_{C1}$-$mGlu4_{C2}$ heterodimer (Ctr) and the indicated mutants induced by different concentrations of VU0155041 with EC_{20} of Glu							
$mGlu2_{C1}$ + $mGlu4_{C2}$ Ctr or mutant		**EC_{50} (μM)**	**EC_{50} ratio**	**pEC_{50} (mean ± s.e.m.)**	**Span (% Ctr)**	**n**	**Expression (% Ctr)**
	Ctr	1.6	1.0	5.80 ± 0.13	100	5	100
TM3	R655A	nd	nd	nd	22 ± 10	5	65 ± 6
	R656A	16.2	10.2	4.79 ± 0.04	110 ± 7	5	82 ± 10
ECL2	K745E	11.0	6.9	4.96 ± 0.07	107 ± 7	4	53 ± 15
	C746A	nd	nd	nd	19 ± 3	3	18 ± 4
	I748A	nd	nd	nd	50 ± 5	4	85 ± 8
TM5	D750A	16.6	10.5	4.78 ± 0.13	57 ± 8	4	113 ± 9
	L753A	nd	nd	nd	72 ± 4	4	86 ± 7
TM6	F805A	nd	nd	nd	72 ± 4	4	109 ± 13

Ca^{2+} release induced by Glu in $mGlu2_{C1}$-$mGlu4_{C2}$ heterodimer (Ctr) or with the mutation SATA						
Ctr or mutant	**EC_{50} (μM)**	**EC_{50} ratio**	**pEC_{50} (mean ± s.e.m.)**	**E_{max} (% Ctr)**	**n**	**Expression (% Ctr)**
						HA **Flag**

$mGlu2_{C1}$ + $mGlu4_{C2}$ (Ctr)	7.1	1.0	5.15 ± 0.05	100	6	100	100
$mGlu2_{C1}$-SATA + $mGlu4_{C2}$	15.8	2.2	4.80 ± 0.07	46 ± 7	5	87 ± 2	70 ± 1
$mGlu2_{C1}$ + $mGlu4_{C2}$-SATA	20.9	3.0	4.68 ± 0.03	61 ± 8	4	113 ± 3	131 ± 5
$mGlu2_{C1}$-SATA + $mGlu4_{C2}$-SATA	5.4	0.8	5.27 ± 0.10	11 ± 48	6	49 ± 3	40 ± 2

Gi activation of $mGlu2_{C1}$-$mGlu4_{C2}$ heterodimer, mGlu2-2 or mGlu4-4 activated by Glu, LY379268 and L-AP4

	Ctr or mutant	EC_{50} (nM)	EC_{50} ratio	pEC_{50} (mean ± s.e.m.)	E_{max} (% Glu)	n	Expression (% mGlu2-2)
mGlu2-4	Glu	3981.1	1.0	5.40 ± 0.12	100	4	105 ± 8
	LY379268	6.3	0.0	8.20 ± 0.05	89 ± 8	4	
	L-AP4	138.0	0.0	6.86 ± 0.08	58 ± 9	4	
mGlu2-2	Glu	3981.1	1.0	5.40 ± 0.07	100	6	100
	LY379268	1.9	0.0	8.73 ± 0.04	93 ± 9	5	
	L-AP4	nd	nd	nd	2 ± 7	5	
mGlu4-4	Glu	7943.3	1.0	5.10 ± 0.05	100	7	93 ± 3
	LY379268	7079.5	0.9	5.15 ± 0.06	87 ± 7	6	
	L-AP4	173.8	0.0	6.76 ± 0.07	98 ± 3	7	

Ca^{2+} release induced by Glu in $mGlu2_{C1}$-$mGlu4_{C2}$ heterodimer (Ctr) or with the FS mutation and co-transfected with Gqi9

	EC_{50} (μM)	EC_{50} ratio	pEC_{50} (mean ± s.e.m.)	E_{max} (% Ctr)	n	Expression (% Ctr) HA	Expression (% Ctr) Flag
$mGlu2_{C1}$ + $mGlu4_{C2}$ (Ctr)	6.5	1.0	5.19 ± 0.02	100	9	100	100
$mGlu2_{C1}$-FS + $mGlu4_{C2}$	7.6	1.2	5.12 ± 0.04	102 ± 8	5	89 ± 5	85 ± 16
$mGlu2_{C1}$ + $mGlu4_{C2}$-FS	nd	nd	nd	5 ± 0	4	114 ± 10	104 ± 15

Ca^{2+} release induced by Glu in $mGlu2_{C1}$-$mGlu4_{C2}$ heterodimer (Ctr) or with the FS mutation and co-transfected with Gqo

	EC_{50} (μM)	EC_{50} ratio	pEC_{50} (mean ± s.e.m.)	E_{max} (% Ctr)	n	Expression (% Ctr) HA	Expression (% Ctr) Flag
$mGlu2_{C1}$ + $mGlu4_{C2}$ (Ctr)	6.8	1.0	5.17 ± 0.04	100	5	100	100
$mGlu2_{C1}$-FS + $mGlu4_{C2}$	7.1	1.0	5.15 ± 0.10	130 ± 4	5	104 ± 3	100 ± 5
$mGlu2_{C1}$ + $mGlu4_{C2}$-FS	nd	nd	nd	-9 ± 4	5	107 ± 5	97 ± 10
$mGlu2_{C1}$-FS + $mGlu4_{C2}$-FS	nd	nd	nd	-14 ± 3	5	109 ± 3	99 ± 3

IP_1 production of $mGlu2_{C1}$-$mGlu4_{C2}$ heterodimer (Ctr) or with mGlu4 mutations

$mGlu2_{C1}$ + $mGlu4_{C2}$ Ctr or mutant	Ctr or mutant	EC_{50} (μM)	EC_{50} ratio	pEC_{50} (mean ± s.e.m.)	Span (% Ctr)	n	Expression (% Ctr)
	Ctr	56.2	1.0	4.25 ± 0.07	100	10	100
ICL1	K619A	nd	nd	nd	18 ± 2	4	96 ± 12
	A620W	nd	nd	nd	21 ± 1	5	50 ± 9
	G622W	nd	nd	nd	10 ± 3	5	31 ± 13
ICL2	G684W	49.0	0.9	4.31 ± 0.17	46 ± 1	3	52 ± 11
	V688A	120.2	2.1	3.92 ± 0.11	48 ± 13	4	137 ± 7
	I694W	nd	nd	nd	21 ± 5	4	36 ± 16
ICL3	F781S	nd	nd	nd	5 ± 2	3	108 ± 19
TM3	R676A	nd	nd	nd	36 ± 3	4	145 ± 13
	I677A	nd	nd	nd	2 ± 6	5	127 ± 16

	R679A	nd	nd	nd	5 ± 2	4	41 ± 19
	I680A	nd	nd	nd	8 ± 3	3	86 ± 9
	F681A	nd	nd	nd	6 ± 7	5	183 ± 11
TM4	P696W	nd	nd	nd	13 ± 6	3	61 ± 14

G protein dissociation induced by Glu on $G\alpha_{i3}$ WT and mutants

$G\alpha_{i3}$-WT or mutant	**EC_{50} (μM)**	**EC_{50} ratio**	**pEC_{50} (mean ± s.e.m.)**	**n**	**Expression (% WT)**
WT	4.6	1.0	5.34 ± 0.2	5	100
I343A	17.0	3.7	4.77 ± 0.17	5	93 ± 4
I344A	6.8	1.5	5.17 ± 0.28	3	104 ± 6
N347A	3.3	0.7	5.48 ± 0.21	3	100 ± 14
L348A	8.7	1.9	5.06 ± 0.26	3	113 ± 11
C351A	4.1	0.9	5.39 ± 0.05	4	123 ± 11
L353A	21.4	4.7	4.67 ± 0.17	3	110 ± 16
Y354A	3.9	0.9	5.41 ± 0.21	3	114 ± 11

Means pEC_{50} were calculated from n independent experiments, and the EC_{50} values were deduced from the mean pEC50. EC_{50} ratio represent the fold shift of EC_{50} calculated by EC_{50}(mutant)/EC_{50}(Ctr) or EC_{50}(mutant)/EC_{50}(WT). n is the number of independent experiments. E_{max} is defined as the maximal agonist response within the concentration range tested. The span is defined as the window between the maximal agonist concentration response and the buffer (no agonist). nd, not determined (data for which a robust concentration response curve or plateau could not be established within the concentration range tested).

Supplementary Table 5. Details of the all-atomistic molecular dynamic simulations.

System Name		mGlu2-4 complex (Pose-1)	mGlu2-4 complex (Pose-2)
System size		10.0×10.0×15.6 nm^3	10.0×10.0×15.6 nm^3
Number of lipids	POPC	232	232
Number of Waters		34,914	34,827
Ions	Na^+	94	94
	Cl^-	115	115

Molecular Dynamics simulations checklist

Reliability and reproducibility checklist for molecular dynamics simulations ***All boxes must be marked YES by acceptance unless an N/A option is available**	**Yes**	**N/A**	**Response** **(Please state where this information can be found in the text)**
1. Convergence of simulations and analysis			
1a. Is an evaluation presented in the text to show that the property being measured has equilibrated in the simulations (*e.g.* time-course analysis)?	☒		Lines 549-551 and Supplementary Fig. 6
1b. Then, is it described in the text how simulations are split into equilibration and production runs and how much data were analyzed from production runs?	☒		Lines 537-540, lines 544-545 and lines 549-551
1c. Are there at least 3 simulations per simulation condition with statistical analysis?	☒		Lines 544-545
1d. Is evidence provided in the text that the simulation results presented are independent of initial configuration?	☒		Lines 544-545
2. Connection to experiments			
2a. Are calculations provided that can connect to experiments (*e.g.* loss or gain in function from mutagenesis, binding assays, NMR chemical shifts, J-couplings, SAXS curves, interaction distances or FRET distances, structure factors, diffusion coefficients, bulk modulus and other mechanical properties, *etc*.)?	☒		Lines 116-118
3. Method choice			
3a. Is it described in the text what force field and water model are used and why?	☒		Lines 534-536
3b. Do simulations contain membranes, membrane proteins, intrinsically disordered proteins, glycans, nucleic acids, polymers, or cryptic ligand binding?	☒	☐	Lines 527-533
If 3b is **YES**, are enhanced sampling methods used?	☐	☒	Response not needed if **N/A**
If enhanced sampling methods are used, are the convergence criteria clearly stated?	☐		
If 3b is **YES**, is it explained in the text why or why not enhanced sampling methods are used?	☒		Lines 544-545 and lines 549-551
4. Code and reproducibility			
4a. Is a table provided describing the system setup, such as simulation box dimensions, total number of atoms, total number of water molecules, salt concentration, lipid composition (number of molecules and type)?	☒		Supplementary Table 5
4b. Is it described in the text what simulation and analysis software and which versions are used?	☒		Lines 535-537, lines 548-549 and lines 557-558
4c. Are initial coordinate and simulation input files and a	☒		Lines 716-719

coordinate file of the final output provided as supplementary files or in a public repository?				
4d. Is there custom code or custom force field parameters?		☐	☒	Response not needed if **N/A**
	If **YES**, are they provided as supplementary profiles or in a public repository?	☐		